

24 **Abstract:** Sensitivity analysis plays an important role in reliability evaluation, structural
25 optimization and structural design, etc. The local sensitivity, i.e., the partial derivative of the
26 quantity of interest in terms of parameters or basic variables, is inadequate when the basic
27 variables are random in nature. Therefore, global sensitivity such as the Sobol' indices based
28 on the decomposition of variance and the moment-independent importance measure, among
29 others, have been extensively studied. However, these indices are usually computationally
30 expensive, and the information provided by them has some limitations for decision making.
31 Specifically, all these indices are positive, and therefore they cannot reveal whether the effects
32 of a basic variable on the quantity of interest are positive or adverse. In the present paper, a
33 novel global sensitivity index is proposed when randomness is involved in structural parameters.
34 Specifically, a functional perspective is firstly advocated, where the probability density function
35 (PDF) of the output quantity of interest is regarded as the output of an operator on the PDF of
36 the source basic random variables. The Fréchet derivative is then naturally taken as a measure
37 for the global sensitivity. In some sense such functional perspective provides a unified
38 perspective on the concepts of global sensitivity and local sensitivity. In the case the change of
39 the PDF of a basic random variable is due to the change of parameters of the PDF of the basic
40 random variable, the computation of the Fréchet-derivative-based global sensitivity index can
41 be implemented with high efficiency by incorporating the probability density evolution method
42 (PDEM) and change of probability measure (COM). The numerical algorithms are elaborated.
43 Several examples are illustrated, demonstrating the effectiveness of the proposed method.

44

45 **Keywords:** uncertainty quantification; global sensitivity index; probability density
46 evolution method; change of probability measure; Fréchet derivative

47 **1 Introduction**

48 A sensitivity index measures, qualitatively or quantitatively, how strong the property of
49 an output quantity of interest (QoI) will change against the change of property of input basic
50 variable(s). Naturally, as the input basic variable(s) are deterministic, the partial derivative of
51 the output QoI in terms of the input basic variable(s) can be naturally adopted as the sensitivity
52 index [1,2], which plays an important role in, e.g., the reliability evaluation [3-8], structural
53 optimization and structural design [9-12], etc. Such sensitivity index, however, is essentially a
54 local sensitivity index and is inadequate if the basic random parameters are random in nature
55 rather than deterministic. In this scenario, some local sensitivity indices may still work well,
56 but a global sensitivity index (GSI) that characterizes global information is also needed, and
57 considerably more informative. In particular, the effects of probability distributions of the input
58 random basic variables should be taken into account.

59 To this end, extensive efforts have been devoted in the past two decades, yielding different
60 formulations for GSI, including the Sobol' index [2,13,14] and the moment-independent
61 importance measure [15-17], among others. The Sobol' index is based on the contribution of a
62 basic variable or basic variable sets to the variance of the output QoI. An orthogonal
63 decomposition of the response surface involving different input basic variables leads to the
64 elegant definition of the Sobol' index [13]. In the past decade, great improvements in the
65 computational efficiency of Sobol' index have been made [18,19]. However, in the Sobol' index,
66 only the variance, i.e., the second-order statistics of the output QoI are involved. This is not
67 sufficiently sensitive, and may even result in a misleading judgment in some cases, e.g., when
68 the probability density function (PDF) of the output QoI has multiple modes [17]. Therefore, it
69 is necessary to develop some kind of GSIs involving the PDF of output QoI. To this kind of
70 GSI belongs the moment-independent importance measure [16], which is defined according to

71 the absolute value of the difference between two different PDFs. Again, computational
72 efficiency becomes an important issue and has been studied in amounts of researches [20].

73 Both the Sobol' type index and the moment-independent index produce positive values.
74 Different from the local sensitivity, they cannot identify the positive or adverse direction, which
75 is an important feature for the selection of direction in structural optimization and decision-
76 making. Actually, an ideal and informative GSI can provide insights or information for the
77 following issues: (1) The order of the importance of source random variables, which can be
78 used to determine whether the uncertainty of some source random variables can be ignored in
79 the detailed model so that the problem can be reduced or simplified; (2) The understanding of
80 global properties of a complex system involving randomness; and (3) The information for the
81 direction and step of iteration in structural design or optimization involving uncertainties. For
82 these purposes, the global sensitivity should provide the magnitude as well as the direction (sign)
83 in a distributed area in the space of the QoI. From the above point of view, the Sobol' index
84 and moment-independent index satisfy the above Issue (1) and partly Issue (2), but not Issue
85 (3). On the other hand, the partial derivative-based sensitivity, i.e., the one related to failure
86 probability in terms of parameters of input random variables, satisfies Issue (3) but does not
87 well satisfy Issues (1) and (2).

88 For this purpose, a novel global sensitivity index is proposed in the present paper. For
89 clarity, a functional perspective to uncertainty propagation is firstly introduced. Then the
90 Fréchet derivative, as a measure of the change of the PDF of the output QoI in terms of the
91 change of the PDF of the input basic variables, is proposed and justified to be an appropriate
92 GSI. Such a functional perspective provides a unified perspective for global and local sensitivity.
93 In the scenario when the change of the PDF of the input source random variables is due to the
94 change of parameters of the distribution, e.g., the mean value or standard deviation, the
95 computational algorithm of GSI is elaborated. In this case, the probability density evolution

96 method (PDEM) is incorporated with the change of probability measure (COM) to provide a
 97 highly efficient approach. Several examples are illustrated, demonstrating the effectiveness of
 98 the proposed method.

99

100 **2 Global Sensitivity Index Based on Fréchet Derivative**

101 *2.1. A Functional Perspective to Uncertainty Propagation in Stochastic System*

102 *Analysis*

103 Without loss of generality, consider a system, of which the output QoI is denoted by X ,
 104 and the input basic variables are denoted by Θ of dimension n . Generally, solving the
 105 underlying physical equation will yield the solution, which means that X is a function of Θ ,
 106 and can be denoted by the following general form

$$107 \quad X = g(\Theta). \quad (1)$$

108 In the present paper, the input basic parameters Θ are regarded as random variables.
 109 Denote the known joint PDF of Θ by $p_{\Theta}(\theta)$. The question arises that how we can capture
 110 the sensitivity of the QoI in terms of the input basic random variable(s).

111 To this end, a functional perspective is firstly advocated. In probability theory, it is well
 112 known that if the PDF of Θ is given, and a function (change of random variable) is determined
 113 by Eq. (1), then the PDF of X can be determined by the rule of change of random variable(s)
 114 [21]. This fact can be expressed in an operator formula

$$115 \quad p_X(x) = \psi(p_{\Theta}(\theta); x) = \psi \circ p_{\Theta}(\theta) \quad (2)$$

116 where ψ is an operator determined by $g(\cdot)$, and \circ means the action of an operator on a
 117 function.

118 Note that ψ is essentially the Frobenius-Perron operator [22]. In fact, the operator
 119 between the output and input PDFs is essentially determined by the underlying physics via the

120 function $g(\cdot)$. In other words, the operator can be regarded as a reflection of the underlying
 121 physics in the ensemble sense.

122

123 2.2. Fréchet-Derivative-Based Global Sensitivity Index

124 It is instructive to compare Eqs. (1) and (2). In Eq. (1), a transformation relation is
 125 established via a function between the input variables and the output QoI, whereas in Eq. (2),
 126 a transformation relation is established via an operator between the PDF of the input variable(s)
 127 and the PDF of the output QoI(s). A natural sensitivity index defined in the context of Eq. (1)
 128 (in particular when the input variable(s) are deterministic) is the partial derivative of the output
 129 QoI in terms of the input basic variable(s). Similarly, in the context of Eq. (2), the sensitivity
 130 index can be defined as an extension of the “partial derivative” of a function in the context of
 131 an operator. The Fréchet derivative provides such an opportunity. In this sense, the functional
 132 perspective provides a unified perspective on the concepts of global sensitivity and local
 133 sensitivity.

134 Consider a small perturbation on the joint PDF of input variables, i.e.,
 135 $p_{\Theta}(\theta) \mapsto p_{\Theta}(\theta) + \delta p_{\Theta}$, where δp_{Θ} is an arbitrary function but satisfying $\int \delta p_{\Theta}(\theta) d\theta = 0$
 136 and $\delta p_{\Theta} > -p_{\Theta}(\theta)$ for $\forall \theta$ to ensure the consistency and non-negativity of PDF. If a linear
 137 bounded operator $F_{\psi} \in L(V, W)$ exists such that [23]

$$138 \lim_{\|\delta p_{\Theta}\|_V \rightarrow 0} \frac{\|\psi(p_{\Theta}(\theta) + \delta p_{\Theta}; x) - \psi(p_{\Theta}(\theta); x) - F_{\psi} \delta p_{\Theta}\|_W}{\|\delta p_{\Theta}\|_V} = 0 \quad (3)$$

139 or equivalently such that

$$140 \psi(p_{\Theta}(\theta) + \delta p_{\Theta}; x) = \psi(p_{\Theta}(\theta); x) + F_{\psi} \delta p_{\Theta} + o(\|\delta p_{\Theta}\|_V), \quad \|\delta p_{\Theta}\|_V \rightarrow 0 \quad (4)$$

141 where $\|\cdot\|_W$ and $\|\cdot\|_V$ are the appropriately equipped norms with respect to p_x and p_{Θ} that
 142 are on the Banach spaces W and V , respectively, then F_{ψ} is the so-called Fréchet

143 derivative of ψ . In the remaining content, all norms are simplified by $\|\cdot\|$ without inducing
 144 confusion.

145 The Fréchet derivative of ψ has a straightforward meaning: when the joint PDF of input
 146 random variables has a tiny perturbation, the PDF of the output QoI will be affected
 147 correspondingly with a certain quantity and direction specified by the Fréchet derivative.
 148 Obviously, this is exactly the natural “sensitivity” of the output QoI in terms of the input
 149 variable(s).

150 **Remark 1.1:** Further, let the probability of failure P_f be

$$151 \quad P_f = \Pr\{X < 0\} = \int_{-\infty}^0 p_X(x)dx = \varphi \circ p_X(x), \quad (5)$$

152 then it is seen that P_f can be regarded as a functional of $p_X(x)$ with the integral operator φ .

153 Similarly, following the rule of change of random variable(s) and Eq. (2), there is

$$154 \quad P_f = \varphi \circ p_X(x) = \varphi \circ \psi(p_{\Theta}(\theta); x) = \phi(p_{\Theta}(\theta)) = \phi \circ p_{\Theta}(\theta) \quad (6)$$

155 and the Fréchet derivative is correspondingly given by

$$156 \quad \lim_{\|\delta p_{\Theta}\| \rightarrow 0} \frac{\|\phi(p_{\Theta}(\theta) + \delta p_{\Theta}) - \phi(p_{\Theta}(\theta)) - F_{\phi} \delta p_{\Theta}\|}{\|\delta p_{\Theta}\|} = 0 \quad (7)$$

157 where F_{ϕ} is a linear operator. It is indicated that the sensitivity of the failure probability can
 158 also be characterized by F_{ϕ} , i.e., the Fréchet derivative with respect to basic distributions of
 159 input variables.

160 **Remark 1.2:** Aside from Eq. (7), we can also define the sensitivity of statistical moments
 161 of QoI. For instance, define the second-order moment of QoI by

$$162 \quad D_X = \int_{-\infty}^{+\infty} x^2 p_X(x)dx = D \circ p_X(x) = D \circ \psi(p_{\Theta}(\theta)) = D \circ p_{\Theta}(\theta) \quad (8)$$

163 then the Fréchet derivative is defined by the linear operator F_D if there exists

$$\lim_{\|\delta p_{\theta}\| \rightarrow 0} \frac{\|D(p_{\theta}(\theta) + \delta p_{\theta}) - D(p_{\theta}(\theta)) - F_d \delta p_{\theta}\|}{\|\delta p_{\theta}\|} = 0. \quad (9)$$

Remark 1.3: In the context of Eq. (1), the sensitivity is defined as the partial derivative of output QoI in terms of the input basic variable(s). Clearly, the PDF of input basic variables is not involved, and the sensitivity is defined at a specified value. In this sense, it is essentially a local sensitivity index. In contrast, in the context of Eq. (2), the sensitivity is defined as the Fréchet derivative, which is the “ratio” of the perturbation of PDF or the perturbation of functional of PDF of the output QoI in terms of the perturbation of PDF of the input variables. Thus, it is defined not on a specified value, but on the whole support of the input variables in terms of the distribution. In this sense, it is a global sensitivity index. The counterparts of local and global sensitivity can be exposed in Table 1.

174

175 **Table 1**

176 Corresponding relationships between the local and global sensitivity

Quantities in the context of local sensitivity	Quantities in the context of global sensitivity
Input deterministic variable(s)	PDF of input random variable(s)
Output QoI	PDF of output QoI as a random variable
Output QoI = function of Input deterministic variable(s)	PDF of output QoI = Operator on/functional of PDF of input random variable(s)
Local sensitivity = the perturbation of output QoI divided by the perturbation of input variable(s)	Global sensitivity = the perturbation of PDF or statistics/failure probability of output QoI divided by the perturbation of PDF of input random variable(s)
Local sensitivity = partial derivative of the function	Global sensitivity = Fréchet derivative of the operator or functional

177

178 In this sense, the global sensitivity index based on the Fréchet derivative can be regarded
 179 as the extension of the local sensitivity. In other words, the above functional perspectives
 180 provide in a sense a unified perspective on the concept of global sensitivity and local sensitivity.

181

182 **3 The Underlying Meaning and Mathematical Expression of the** 183 **Fréchet-Derivative-based GSI for Stochastic Systems**

184 *3.1. The Expressions of GSI based on the Fréchet Derivative and Gâteaux Derivative*

185 The Fréchet derivative can be related to the Gâteaux derivative, which is a generalization
 186 of the classical directional derivative, defined by [24]

$$187 \lim_{|\varepsilon| \rightarrow 0} \frac{\psi(p_{\theta}(\theta) + \varepsilon \delta p_{\theta}; x) - \psi(p_{\theta}(\theta); x)}{\varepsilon} = \mathbf{G}_{\psi} \delta p_{\theta}, \quad \forall \delta p_{\theta} \in V, \quad (10)$$

188 if there exists such an operator $\mathbf{G}_{\psi} \in \mathbf{L}(V, W)$, where the operator $\psi : K \subset V \rightarrow W$ is defined
 189 between two Banach spaces. Specifically, the Gâteaux derivative at $p_{\theta}(\theta)$ is identical to the
 190 Fréchet derivative, if the limit in Eq. (10) is uniform with respect to δp_{θ} with $\|\delta p_{\theta}\|=1$ or
 191 if the Gâteaux derivative is continuous at $p_{\theta}(\theta)$. This property makes it possible to compute
 192 the Fréchet derivative according to the definition of the Gâteaux derivative [24,25]. Thus, the
 193 proposed GSI in Eqs. (3) and (4) can be redefined by Eq. (10) with a well-defined norm, e.g.,

$$194 \|p\|_V = \frac{1}{2} \|p\|_{L^1(\Omega_{\theta})} \quad (11)$$

195 where the norm $\|\cdot\|_V$ is defined by the half of L^1 -norm, i.e.,

$$196 \|p\|_V = \frac{1}{2} \int_{\Omega_{\theta}} |p| d\theta \quad (12)$$

197 which is exactly the so-called *total variation distance* [28].

198 To provide more insight into the physical/geometrical meaning and to provide a pragmatic
 199 computational approach, the expression of the Fréchet-derivative-based GSI will then be
 200 elaborated in the following subsections for different cases.

201

202 3.2. *Case of Discrete Distributions*

203 The meaning of Fréchet-derivative-based GSI can be seen much more clearly when the
 204 input distributions are of the discrete type. For clarity, let us first consider the case when the
 205 input variable in Eq. (1) is a random variable Θ , i.e.,

206
$$X = g(\Theta). \quad (13)$$

207 Let the sample space be a finite and countable set $\{\theta_i\}_{i=1}^N$ on Ω , such that

208
$$\mathbf{P}\{\Theta = \theta_i\} = \mathbf{P}_{\Theta}^{(i)} \geq 0 \text{ and } \sum_{i=1}^N \mathbf{P}_{\Theta}^{(i)} = 1 \quad (14)$$

209 where $\mathbf{P}(\cdot)$ denotes the probability of a random event.

210 The physical relation in Eq. (13) gives the following mapping

211
$$x_k = g\left(\theta_{\{i\}_k}\right), k = 1, 2, \dots, M \text{ with } \{i\}_k \subseteq \{1, 2, \dots, N\} \quad (15)$$

212 where $\{i\}_p \cap \{i\}_q = \emptyset$ for $\forall p \neq q$ and $\cup_{k=1}^M \{i\}_k = \{1, 2, \dots, N\}$. This means that for all

213 $j \in \{i\}_k$, there is $x_k = g(\theta_j)$ yielding the same value x_k . In other words, for all the input

214 values in the subset $\{\theta_j\}_{j \in \{i\}_k}$, the output values are identical. Denote the cardinal number of

215 the subset $\{i\}_k$ by n_k , i.e., $n_k = \text{card}(\{i\}_k) \geq 1$. Obviously, there is $M \leq N$ and $\sum_{k=1}^M n_k = N$

216 due to the many-to-one mapping.

217 Denote the probability mass function of output by

218
$$\mathbf{P}\left\{x = x_k = g\left(\theta_{\{i\}_k}\right)\right\} = \mathbf{P}_X^{(k)} \geq 0, k = 1, 2, \dots, M \text{ with } \{i\}_k \subseteq \{1, 2, \dots, N\}. \quad (16)$$

219 Then according to Eq. (15) we have

220
$$\mathbf{P}_X^{(k)} = \sum_{j \in \{i\}_k} \mathbf{P}_{\Theta}^{(j)}, k = 1, 2, \dots, M. \quad (17)$$

221 For convenience, denote the probability measure of Θ be a vector

222 $\mathbf{P}_\Theta = \left(\mathbf{P}_\Theta^{(1)}, \mathbf{P}_\Theta^{(2)}, \dots, \mathbf{P}_\Theta^{(N)} \right)^\top$ and that of X by a vector $\mathbf{P}_X = \left(\mathbf{P}_X^{(1)}, \mathbf{P}_X^{(2)}, \dots, \mathbf{P}_X^{(M)} \right)^\top$. Then, Eq.

223 (17) can be rewritten in a matrix form by

$$224 \quad \mathbf{P}_X = \mathbf{F}_{M \times N} \mathbf{P}_\Theta \quad (18)$$

225 where the matrix $\mathbf{F}_{M \times N}$ is a Boolean matrix whose element is either 1 or 0. According to Eq.

226 (16), it is easy to determine the value of the components F_{kj} of the matrix $\mathbf{F}_{M \times N}$,

$$227 \quad F_{kj} = I(j \in \{i\}_k) \quad (19)$$

228 for $k = 1, 2, \dots, M; j = 1, 2, \dots, N$, where $I(\cdot)$ is the indicator with the value being one if the

229 event is true and otherwise zero. It is seen clearly that, for the case of many-to-one mapping, in

230 each column only one element is valued 1 and all the other elements are valued zero, but in

231 each row, there are at least one and possibly more elements valued 1. Actually, in the k -th row

232 of $\mathbf{F}_{M \times N}$, the number of elements valued 1 is $n_k = \text{card}(\{i\}_k) \geq 1$.

233 By doing so, Eq. (18) can be rewritten in a component form more explicitly

$$234 \quad \mathbf{P}_X^{(k)} = \sum_{j=1}^N F_{kj} \mathbf{P}_\Theta^{(j)} = \sum_{j=1}^N I(j \in \{i\}_k) \mathbf{P}_\Theta^{(j)}, \quad k = 1, 2, \dots, M. \quad (20)$$

235 Further, denoting $\mathbf{P}_X = \mathbf{F}_{M \times N} \mathbf{P}_\Theta = \mathbf{G}(\mathbf{P}_\Theta)$, it is easy to find that

$$236 \quad \mathbf{G}(\mathbf{P}_\Theta + \delta \mathbf{P}_\Theta) = \mathbf{F}_{M \times N} (\mathbf{P}_\Theta + \delta \mathbf{P}_\Theta) = \mathbf{F}_{M \times N} \mathbf{P}_\Theta + \mathbf{F}_{M \times N} \delta \mathbf{P}_\Theta = \mathbf{G}(\mathbf{P}_\Theta) + \mathbf{F}_{M \times N} \delta \mathbf{P}_\Theta \quad (21)$$

237 where $\delta \mathbf{P}_\Theta$ is a variation of the vector \mathbf{P}_Θ , or alternatively

$$238 \quad \lim_{\varepsilon \rightarrow 0} \frac{\mathbf{G}(\mathbf{P}_\Theta + \varepsilon \delta \mathbf{P}_\Theta) - \mathbf{G}(\mathbf{P}_\Theta)}{\varepsilon} = \lim_{\varepsilon \rightarrow 0} \frac{\mathbf{F}_{M \times N} (\mathbf{P}_\Theta + \varepsilon \delta \mathbf{P}_\Theta) - \mathbf{F}_{M \times N} \mathbf{P}_\Theta}{\varepsilon} = \mathbf{F}_{M \times N} \delta \mathbf{P}_\Theta \quad (22)$$

239 which means that according to the definition in Eqs. (4) or (10), the Boolean matrix $\mathbf{F}_{M \times N}$ is

240 nothing but the Fréchet derivative in the case of discrete distributions.

241 Further, by denoting the variation of the vector \mathbf{P}_X by

242 $\delta\mathbf{P}_X = \delta\mathbf{G}(\mathbf{P}_\Theta) = \mathbf{G}(\mathbf{P}_\Theta + \delta\mathbf{P}_\Theta) - \mathbf{G}(\mathbf{P}_\Theta)$, then there is

$$243 \quad \delta\mathbf{P}_X = \mathbf{F}_{M \times N} \delta\mathbf{P}_\Theta. \quad (23)$$

244 This means that once the Fréchet derivative is known, then the variation of the output
 245 probability mass function can be obtained directly from the variation of input probability mass
 246 function. Actually, this is consistent with the discussion of global sensitivity in [Table 1](#). Also,
 247 from this expression, it is clear to see that the Fréchet derivative for the case of discrete
 248 distribution is a linear operator.

249 Now the underlying meaning of the Fréchet-derivative-based GSI becomes apparent:
 250 every element of value 1 in the Boolean matrix $\mathbf{F}_{M \times N}$ means the physical relation in Eq. (15)
 251 holds, and thus the probability measure can be propagated from the input distribution \mathbf{P}_Θ to
 252 the distribution \mathbf{P}_X of output QoI X . The sensitivity of the stochastic system strictly follows
 253 the physical pathway! Also, it is seen clearly that Eq. (23) is an extended version of the
 254 differentiation of a function.

255 To be more intuitive, consider a simple example. Let $X = \Theta^2$ and $\Theta \in \{-1, 0, 1\}$ with
 256 $\mathbf{P}_\Theta = (1/6, 1/3, 1/2)^\top$. It is easy to know that $X \in \{0, 1\}$ with $\mathbf{P}_X = (1/3, 2/3)^\top$ by
 257 admitting $\mathbf{P}_X = \mathbf{F}_{2 \times 3} \mathbf{P}_\Theta$ where

$$258 \quad \mathbf{F}_{2 \times 3} = \begin{bmatrix} 0 & 1 & 0 \\ 1 & 0 & 1 \end{bmatrix} \quad (24)$$

259 is the Fréchet derivative. Clearly, it is a Boolean matrix that follows Eq. (19). Further, if there
 260 is a variation in \mathbf{P}_Θ , e.g., $\delta\mathbf{P}_\Theta = (-1/12, -1/12, 1/6)^\top$, by substituting Eq. (24) in Eq. (23)
 261 we have $\delta\mathbf{P}_X = \mathbf{F}_{2 \times 3} \delta\mathbf{P}_\Theta = (-1/12, 1/12)^\top$, and therefore the updated probability mass vector

262 is $\mathbf{P}'_{\bar{X}} = \mathbf{P}_{\bar{X}} + \delta \mathbf{P}_X = (1/4, 3/4)^\bullet$. This result is, of course, consistent with the result of Eqs. (18)

263 and (21) such that $\mathbf{P}'_{\bar{X}} = \mathbf{F}_{2 \times 3} \mathbf{P}'_{\Theta}$ where $\mathbf{P}'_{\Theta} = \mathbf{P}_{\Theta} + \delta \mathbf{P}_{\Theta} = (1/12, 1/4, 2/3)^\bullet$.

264 In the case the input in Eq. (1) is a random vector $\Theta = (\Theta_1, \Theta_2, \dots, \Theta_n)^\bullet$, if the sampling

265 space is still a discrete set, e.g., $\{(\theta_{i_1}, \theta_{i_2}, \dots, \theta_{i_n})^\bullet\}_{i_1=1,2,\dots,N_1; \dots, i_n=1,2,\dots,N_n}$, where N_j denotes the

266 number of realizable values of Θ_j , then a one-dimensional array can be adopted to store the

267 values in the sampling space. For instance, we may denote $\theta_k = (\theta_{i_1}, \theta_{i_2}, \dots, \theta_{i_n})^\bullet$, where a one

268 to one map between k and the array (i_1, i_2, \dots, i_n) can be established, e.g., by

$$269 \quad k = (i_1 - 1)N_2 \cdots N_n + (i_2 - 1)N_3 \cdots N_n + (i_{s-1} - 1)N_n + i_n = \sum_{j=1}^{n-1} (i_j - 1) \prod_{m=j+1}^n N_m + i_n. \quad (25)$$

270 Then a vector can be used to denote the probability mass function, and thus the ideas in

271 the present section for a random variable input can be adopted and similar deductions can be

272 carried out. This will not be detailed here to avoid lengthiness of the paper.

273

274 3.3. Case of Continuous Distributions

275 3.3.1. General Expression

276 When the input distributions of discrete type tend to be continuous, things are getting much

277 more interesting but also much more involved. Denote the input PDF of Θ by $p_{\Theta}(\theta)$ and

278 the output PDF of X by $p_X(x)$, then Eq. (18) should be extended to

$$279 \quad p_X(x) = \int_{\Omega_{\Theta}} \delta_D(x - g(\theta)) p_{\Theta}(\theta) d\theta \quad (26)$$

280 where $\delta_D(\cdot)$ denotes the Dirac function to avoid possible confusion between the variation of

281 a function and the Dirac function. By the definition of Fréchet derivative, if there is a variation

282 in the input PDF δp_{Θ} , one can easily notice that

$$\begin{aligned}
\psi(p_{\Theta} + \delta p_{\Theta}) &= \int_{\Omega_{\Theta}} \delta_D(x - g(\theta))(p_{\Theta} + \delta p_{\Theta}) d\theta \\
&= \int_{\Omega_{\Theta}} \delta_D(x - g(\theta)) p_{\Theta} d\theta + \int_{\Omega_{\Theta}} \delta_D(x - g(\theta)) \delta p_{\Theta} d\theta \\
&= \psi(p_{\Theta}) + F_{\psi} \circ \delta p_{\Theta}
\end{aligned} \tag{27}$$

where ψ is the integral operator defined in Eq. (26) and F_{ψ} is the Fréchet derivative of ψ . Since ψ is a linear operator, the Fréchet derivative of ψ is nothing but itself [24]. This is consistent with the case involving discrete distributions.

Moreover, by the definition of Gâteaux derivative, it can be easily proved that

$$\begin{aligned}
&\lim_{\varepsilon \rightarrow 0} \frac{\psi(p_{\Theta} + \varepsilon \delta p_{\Theta}) - \psi(p_{\Theta})}{\varepsilon} \\
&= \lim_{\varepsilon \rightarrow 0} \frac{\int_{\Omega_{\Theta}} \delta_D(x - g(\theta))(p_{\Theta} + \varepsilon \delta p_{\Theta}) d\theta - \int_{\Omega_{\Theta}} \delta_D(x - g(\theta)) p_{\Theta} d\theta}{\varepsilon} \\
&= \int_{\Omega_{\Theta}} \delta_D(x - g(\theta)) \delta p_{\Theta} d\theta \text{ for } \forall \delta p_{\Theta} \in V
\end{aligned} \tag{28}$$

where one can see that the Boolean matrix in Eq. (21) or (22), i.e., the Fréchet derivative for the discrete case, turns to be the integral operator in terms of the Dirac function $\delta_D(\cdot)$ as presented in Eq. (27) or (28), which is apparently reasonable: the selection property of the Dirac function works exactly the same as the logic calculation of the Boolean element (1 or 0), and the summation calculation evolves into the integral calculation when the system becomes continuous.

Further, if we denote $\delta p_X = \delta \psi(p_{\Theta}) = \psi(p_{\Theta} + \delta p_{\Theta}) - \psi(p_{\Theta})$, then from Eq. (26) there is

$$\delta p_X = \int_{\Omega_{\Theta}} \delta_D(x - g(\theta)) \delta p_{\Theta} d\theta = F_{\psi} \circ \delta p_{\Theta}. \tag{29}$$

Similar to the cases involving discrete distributions, this expression means that once the Fréchet derivative is known, then the variation of the output PDF can be obtained directly from the variation of the input PDF. Again, this justifies the appropriation of taking the Fréchet derivative as a global sensitivity index, as shown in Table 1.

302 A more explicit expression for Eq. (28) by integrating in terms of the Dirac function yields

$$\begin{aligned}
\delta p_X &= \int_{\Omega_{\theta}} \delta_D(x - g(\theta)) \delta p_{\theta} d\theta \\
303 \quad &= \int_{\Omega_{\theta_{\square 1}}} \sum_{j=1}^R \left(\left| \frac{\partial g(\theta_1; \theta_{\square 1})}{\partial \theta_1} \right|^{-1} \delta p_{\theta} \right)_{\theta_1 = g_j^{-1}(x; \theta_{\square 1})} d\theta_{\square 1} \quad (30) \\
&= F_{\psi} \circ \delta p_{\theta}
\end{aligned}$$

304 where $\theta_{\square 1} = (\theta_2, \theta_3, \dots, \theta_n)$, $\theta_1 = g_j^{-1}(x; \theta_{\square 1})$ is the j -th inverse function of g for fixed $\theta_{\square 1}$, R is
305 the number of inverse function when the function of g for fixed $\theta_{\square 1}$ is non-monotonic. This
306 expression, though usually unfeasible for practical computation, is theoretically important. It
307 again shows that the Fréchet derivative is a linear operator, connects the variation of input PDF
308 and the variation of output PDF, and can thus be in principle an appropriate global sensitivity
309 index.

310

311 3.3.2. Parametric Expression

312 Generally, in many practical engineering cases, the distribution type is determined while
313 the distribution parameters, e.g., the mean value μ and standard deviation σ in Gaussian
314 or lognormal distributions, or the shape and shift parameters in Weibull distribution, may vary
315 due to data sparsity, information updating, etc. For simplicity of writing, denote the distribution
316 parameters by a vector $\xi = (\xi_1, \dots, \xi_m)^T$, where m is the total number of distribution parameters,
317 then the Fréchet derivative defined by Eq. (3) becomes

$$318 \quad F_{\psi}(x) = \frac{\partial F(x; \xi) / \partial \xi}{\|\partial p_{\theta}(\theta; \xi) / \partial \xi\|} = \left(\frac{\partial p_X(x; \xi) / \partial \xi_1}{\|\partial p_{\theta}(\theta; \xi) / \partial \xi_1\|_V}, \dots, \frac{\partial p_X(x; \xi) / \partial \xi_m}{\|\partial p_{\theta}(\theta; \xi) / \partial \xi_m\|_V} \right)^T \quad (31)$$

319 where

$$320 \quad F(x; \xi) = \psi(p_{\theta}(\theta; \xi)) = \psi \circ p_{\theta}(\theta; \xi). \quad (32)$$

321 According to the consistency between the Fréchet derivative and the Gâteaux derivative in

322 Eq. (10), we have

$$323 \quad F_{\psi} \tilde{\delta} p_{\Theta} = \lim_{\varepsilon \rightarrow 0} \frac{\psi(p_{\Theta} + \varepsilon \tilde{\delta} p_{\Theta}) - \psi(p_{\Theta})}{\varepsilon} \quad (33)$$

324 where $\|\tilde{\delta} p_{\Theta}\|_V = 1$, $\delta p_{\Theta} = \tilde{\delta} p_{\Theta} / \varepsilon$ is a standardized variation for $\varepsilon > 0$, and δp_{Θ} is the
 325 variation of input PDF satisfying $\int \delta p_{\Theta} d\theta = 0$ and $\delta p_{\Theta} > -p_{\Theta}(\theta)$. Noticing that the
 326 variation of input PDF is

$$327 \quad \delta p_{\Theta}(\theta; \xi_1, \dots, \xi_m) = p_{\Theta}(\theta; \xi + \delta \xi) - p_{\Theta}(\theta; \xi) = \sum_{j=1}^m \frac{\partial p_{\Theta}(\theta; \xi_1, \dots, \xi_m)}{\partial \xi_j} \delta \xi_j. \quad (34)$$

328 There is

$$329 \quad \|\tilde{\delta} p_{\Theta}\|_V = \|(p_{\Theta}(\theta; \xi + \delta \xi) - p_{\Theta}(\theta; \xi)) / \varepsilon\|_V = 1, \quad (35)$$

330 or alternatively,

$$331 \quad \varepsilon = \|p_{\Theta}(\theta; \xi + \delta \xi) - p_{\Theta}(\theta; \xi)\|_V. \quad (36)$$

332 Therefore,

$$\begin{aligned} & \lim_{|\varepsilon| \rightarrow 0} \frac{\psi(p_{\Theta}(\theta) + \varepsilon \tilde{\delta} p_{\Theta}; x) - \psi(p_{\Theta}(\theta); x)}{\varepsilon} \\ 333 \quad &= \lim_{|\delta \xi| \rightarrow 0} \frac{\psi(p_{\Theta}(\theta; \xi + \delta \xi); x) - \psi(p_{\Theta}(\theta); x)}{\|p_{\Theta}(\theta; \xi + \delta \xi) - p_{\Theta}(\theta; \xi)\|_V} \quad (37) \\ &= \lim_{|\delta \xi| \rightarrow 0} \sum_{j=1}^m \left(\frac{\partial p_X(x; \xi)}{\partial \xi_j} \right) \delta \xi_j \left/ \left\| \sum_{j=1}^m \left(\frac{\partial p_{\Theta}(\theta; \xi)}{\partial \xi_j} \right) \delta \xi_j \right\|_V \right. \end{aligned}$$

334 Notice that if, without loss of generality, we further consider the situation $\delta \xi_j$'s are
 335 independent variation, and any component of the Fréchet derivative can be obtain from the
 336 above equation by letting $\delta \xi_j \neq 0$ whereas all the other variations are zero, i.e.,

$$337 \quad F_{\psi, j} = \frac{\partial p_X(x; \xi) / \partial \xi_j}{\|\partial p_{\Theta}(\theta; \xi) / \partial \xi_j\|_V}, \quad j = 1, 2, \dots, m \quad (38)$$

338 which is nothing but the result in Eq. (31).

339 It is interesting that the difference between the Fréchet derivative and the usual partial
 340 derivative in the parametric case is that there is a normalization factor. This is important,
 341 because this naturally occurred normalization factor eliminates the effect of dimensionality of
 342 different parameters.

343 In this case, the propagation of uncertainty as exhibited by the effects of variation of input
 344 probabilistic information on the output probabilistic information becomes

$$345 \begin{aligned} \delta p_X(x; \xi) &= p_X(x; \xi + \delta \xi) - p_X(x; \xi) \\ &= F_\nu \circ \delta \tilde{\xi} \end{aligned} \quad (39)$$

346 where $\delta \tilde{\xi}$ is the normalized or dimensionless variation of parametric vector

$$347 \delta \tilde{\xi} = \left(\frac{\delta \xi_1}{\|\partial p_\theta(\theta; \xi)/\partial \xi_1\|_V}, \frac{\delta \xi_2}{\|\partial p_\theta(\theta; \xi)/\partial \xi_2\|_V}, \dots, \frac{\delta \xi_m}{\|\partial p_\theta(\theta; \xi)/\partial \xi_m\|_V} \right)^T. \quad (40)$$

348 It is easy to prove Eq. (39) as follows

$$349 \begin{aligned} \delta p_X(x; \xi) &= p_X(x; \xi + \delta \xi) - p_X(x; \xi) \\ &= \int_{\Omega_\theta} \delta_D(x - g(\theta)) \left(\sum_{j=1}^m \frac{\partial p_\theta(\theta; \xi_1, \dots, \xi_m)}{\partial \xi_j} \delta \xi_j \right) d\theta \\ &= \sum_{j=1}^m \left(\frac{\partial}{\partial \xi_j} \int_{\Omega_\theta} \delta_D(x - g(\theta)) p_\theta(\theta; \xi_1, \dots, \xi_m) d\theta \right) \delta \xi_j \\ &= \sum_{j=1}^m \left(\frac{\partial p_X(x; \xi_1, \dots, \xi_m)/\partial \xi_j}{\|\partial p_\theta(\theta; \xi)/\partial \xi_j\|_V} \right) \tilde{\delta \xi}_j \\ &= F_\nu \circ \delta \tilde{\xi}. \end{aligned} \quad (41)$$

350 On this condition, the Fréchet derivative reduces to a normalized version of “ordinary
 351 derivative”. For instance, if the change of PDF of input basic random variables is due to change
 352 of the mean of input basic random variables, then Eq. (31) further reduces to

$$353 F_\nu(x) = \frac{\partial F(x; \mu)/\partial \mu}{\|\partial p_\theta(\theta; \mu)/\partial \mu\|_V} \quad (42)$$

354 where $\boldsymbol{\mu}$ is the vector of mean value of the input random variables, and it is easy to verify
355 that

$$356 \int_{-\infty}^{\infty} \mathbf{F}_{\psi}(x) dx = 0 \quad (43)$$

357 which means that, if the Fréchet derivative in Eq. (42) is not always be zero at all x , then it
358 cannot be always positive nor always negative, but must be positive in some areas and negative
359 in the rest areas in terms of x . In other words, the curve of the Fréchet derivative must have at
360 least one additional point crossing the abscissa besides the left and right end points. This
361 property can be adopted as a qualitative property for the verification of analytical or numerical
362 results.

363 Note that the sensitivity index in Eq. (42) is computed for the whole PDF of X , even
364 for a specified value of $\boldsymbol{\mu}$. In this sense, even the sensitivity in Eq. (42) reduces to a normalized
365 “usual” partial derivative, it is a global sensitivity index.

366 Generally, the calculation of the norm term in Eqs. (31) and (42) is quite simple, since
367 there exist analytical results (available in Appendix B for some common distributions), but the
368 computation of the partial term defined in Eq. (31) or (42) requires multiple rounds of
369 stochastic response analysis (or reliability evaluation), and in each round of stochastic analysis
370 multiple, say, for different problems in the order of magnitude of 10^3 to 10^8 in Monte Carlo
371 simulation, deterministic function evaluations are needed. This leads to prohibitively large
372 computational efforts. Incorporating the probability density evolution method (PDEM) and the
373 change of probability measure (COM) [26], a highly efficient algorithm can be implemented
374 and will be elaborated in the following sections.

375

376 **4 Numerical Algorithm for Fréchet-Derivative-based GSI**

377 In order to evaluate the proposed GSI in Eq. (31), the numerical algorithm is discussed in
378 terms of Gâteaux derivative presented in Section 4.1. Besides, the probability density evolution

379 method (PDEM) and the change of probability measure (COM) are incorporated. To be clear,
 380 the pivotal theories and numerical algorithms for PDEM and COM are firstly summarized in
 381 [Section 4.2 and 4.3](#), respectively. Then, the complete numerical algorithm for the Fréchet-
 382 derivative-based GSI is elaborated in [Section 4.4](#).

383

384 *4.1. The Basic Idea of Numerical Algorithm in terms of Gâteaux Derivative*

385 In numerical implementation, the Gâteaux derivative usually takes advantage in
 386 computation over the Fréchet derivative. Therefore, the basic idea of numerical algorithm to
 387 generate the Fréchet derivative is to take advantage of the evaluation of Gâteaux derivative,
 388 which requires the following two assumptions [25]: (1) the Gâteaux derivative is continuous at
 389 $p_{\Theta}(\boldsymbol{\theta})$, and (2) the variation of input PDF is unit, i.e., $\|\tilde{\delta} p_{\Theta}\|_V = 1$.

390 Moreover, by denoting the variation of input PDF as

$$391 \quad \tilde{p}_{\Theta}(\boldsymbol{\theta}) = p_{\Theta}(\boldsymbol{\theta}) + \varepsilon \tilde{\delta} p_{\Theta}, \quad (44)$$

392 we immediately have

$$393 \quad \|\tilde{p}_{\Theta}(\boldsymbol{\theta}) - p_{\Theta}(\boldsymbol{\theta})\|_V = \|\varepsilon \tilde{\delta} p_{\Theta}\|_V = \varepsilon \quad (45)$$

394 where ε is an infinitesimal number defined in Eq. (10). In practical computation, ε can be
 395 taken as a small value, e.g., $\varepsilon = 0.01$, and then the Gâteaux derivative can be approximated by

$$396 \quad \mathbf{G}_V \approx \frac{\psi(\tilde{p}_{\Theta}(\boldsymbol{\theta}); x) - \psi(p_{\Theta}(\boldsymbol{\theta}); x)}{\varepsilon} \quad (46)$$

397 where $\tilde{p}_{\Theta}(\boldsymbol{\theta})$ is an arbitrary PDF satisfying Eq. (45). The basic idea of numerical algorithm
 398 for the evaluation of Gâteaux derivative is then summarized as below:

399 **Step 0.1.** Set ε to be a small value, e.g., $\varepsilon = 0.01$;

400 **Step 0.2.** Find one proper PDF $\tilde{p}_{\Theta}(\boldsymbol{\theta})$ satisfying Eq. (45).

401 **Step 0.3.** Calculate Eq. (46).

402 In **Step 0.3** required is the evaluation of $\psi(\tilde{p}_\Theta(\theta); x)$ and $\psi(p_\Theta(\theta); x)$, which is
403 usually time-consuming. To efficiently and accurately compute these two quantities, the
404 probability density evolution method (PDEM) combined with the change of probability
405 measure (COM) [26] (PDEM-COM) is adopted hereafter, where PDEM (introduced in [Sections](#)
406 [4.2](#)) is utilized to evaluate $\psi(p_\Theta(\theta); x)$ while COM (summarized in [Sections 4.3](#)) is adopted
407 to compute $\psi(\tilde{p}_\Theta(\theta); x)$. The PDF found in **Step 0.2** is not numerically unique, therefore the
408 parametric form in [Section 3.3.2](#) is taken into account. It should be emphasized that introducing
409 parametric distributions will not change the properties of the proposed Fréchet-derivative-based
410 GSI, according to the **Proposition** in [Appendix A](#).

411

412 *4.2. Uncertainty Propagation via Probability Density Evolution Method (PDEM)*

413 For clarity, consider a one-dimensional stochastic dynamical system:

$$414 \quad \dot{X} = G(X, \Theta, t), \quad X(t_0) = X_0 \quad (47)$$

415 where Θ is a random vector with joint PDF $p_\Theta(\theta)$ characterizing the source of randomness
416 involved in the system, and X_0 is the initial value. Obviously, for a well-posed system, the
417 solution of Eq. (47) uniquely exists, and is continuously dependent on Θ and X_0 . Without
418 loss of generality, the solution is assumed to take the form

$$419 \quad X = H(X_0, \Theta, t). \quad (48)$$

420 Moreover, the derivative of X with respect to time t can be written as

$$421 \quad \dot{X} = h(X_0, \Theta, t) \quad (49)$$

422 where $h(\cdot) = \partial H(\cdot) / \partial t$, and \dot{X} is the generalized velocity. In [27], it is elaborated that, if
423 there is no existent random factors disappear, nor new random factors arise, the system will be

424 probability preserved. Accordingly, a generalized density evolution equation (GDEE) can be
 425 derived as [28]

$$426 \quad \frac{\partial p_{x\Theta}(x, \boldsymbol{\theta}, t)}{\partial t} + h(\boldsymbol{\theta}, t) \frac{\partial p_{x\Theta}(x, \boldsymbol{\theta}, t)}{\partial x} = 0 \quad (50)$$

427 where the initial value X_0 in Eq. (50) is omitted without inducing confusion. The
 428 corresponding initial condition is

$$429 \quad p_{x\Theta}(x, \boldsymbol{\theta}, t_0) = \delta_D(x - H(\boldsymbol{\theta}, t_0)) \cdot p_{\Theta}(\boldsymbol{\theta}) \quad (51)$$

430 where $\delta_D(\cdot)$ is the Dirac function.

431 The PDEM is adopted herein due to its efficiency and flexibility in the analysis of
 432 uncertainty propagation, which has been validated in [29]. In general, the solution procedure of
 433 PDEM includes the following four steps:

434 **Step 1.1.** Partition the probability space by a set of optimally selected points, of which the
 435 GF-discrepancy of point set is minimized [30,31]. Denote the optimal point set by

$$436 \quad M = \left\{ \boldsymbol{\theta}_q, P_q \right\}_{q=1}^{n_{\text{sel}}}, \text{ where } \boldsymbol{\theta}_q \text{ is the } q\text{-th representative points with corresponding assigned}$$

437 probability $P_q = \int_{\Omega_q} p_{\Theta}(\boldsymbol{\theta}) d\boldsymbol{\theta}$, n_{sel} is the total number of the representative points. Here Ω_q

438 stands for the representative domain specified by the Voronoi cell [32]. Note that if Θ is a

439 high-dimensional vector, some appropriate dimension-reduction strategies should be utilized,

440 e.g., the mapping method [33] and the active subspace method [34], etc.

441 **Step 1.2.** For each $\Theta = \boldsymbol{\theta}_q$, solve Eq. (47) to yield the corresponding \dot{X}_q or $h(\boldsymbol{\theta}_q, t)$.

442 **Step 1.3.** For each $\Theta = \boldsymbol{\theta}_q$, solve Eq. (50) and get $p_{x\Theta}^{(q)}$ for $q = 1, \dots, n_{\text{sel}}$. Notice that the

443 initial condition of Eq. (51) now becomes $p_{x\Theta}^{(q)}(x, \boldsymbol{\theta}, t_0) = \delta_D(x - x_0) P_q$. Since Eq. (50) is a

444 typical hyperbolic partial differential equation, the finite difference method (FDM) is adopted.

445 Moreover, in order to tradeoff the dissipation and dispersion in numerical computation, the
 446 TVD (Total Variation Diminishing) scheme is suggested [35].

447 **Step 1.4.** Assemble all the solutions in **Step 1.3** to yield the PDF of X , i.e.,

$$448 \quad p_X(x, t) = \int_{\Omega_{\Theta}} p_{X\Theta}(x, \theta, t) d\theta \square \sum_{q=1}^{n_{\text{sel}}} p_{X\Theta}^{(q)}(x, \theta_q, t) \quad \text{where } \Omega_{\Theta} = \cup_{q=1}^{n_{\text{sel}}} \Omega_q.$$

449

450 4.3. Change of Probability Measure (COM) and Radon-Nikodym Derivative

451 After performing one round of PDEM analysis for a specified joint PDF of source basic
 452 random variables, if it is found that the joint PDF of source basic random variables should be
 453 changed to some other joint PDF, say, due to the epistemic uncertainty [26], then a completely
 454 new round of PDEM analysis is needed. The new round of PDEM analysis will of course make
 455 the previous round of PDEM analysis totally invalid. Most recently, the change of probability
 456 measure (COM) by the Radon-Nikodym derivative was incorporated with PDEM to expedite
 457 the procedure of uncertainty propagation in the case the joint PDF of source basic random
 458 variables is changed. In the PDEM-COM, the most time-consuming underlying deterministic
 459 analyses in PDEM in **Step 1.2** [26] are re-used. The basic idea is as follows:

460 Consider two close but different distributions of Θ , denoted as $p_{\Theta}^{(1)}(\theta)$ and $p_{\Theta}^{(2)}(\theta)$,
 461 respectively. If Eq. (47) holds, the corresponding PDF for the response X can be firstly
 462 calculated by one round of PDEM analysis in terms of $p_{\Theta}^{(1)}(\theta)$, and thus $p_X^{(1)}(x)$ is obtained.
 463 For the case of $p_X^{(2)}(x)$ with respect to $p_{\Theta}^{(2)}(\theta)$, instead of doing another complete round of
 464 PDEM analysis, the Radon-Nikodym operator [21], denoted as $T_{2,1}$, is advocated such that

$$465 \quad p_X^{(2)}(x) = T_{2,1} p_X^{(1)}(x). \quad (52)$$

466 The approach presented in [26] is then summarized as the following three steps:

467 **Step 2.1.** For a certain $p_{\Theta}^{(1)}(\theta)$, accomplish one round of PDEM analysis, as shown in
 468 [Section 4.2](#). Denote the point set as $M^{(1)} = \{\theta_q^{(1)}, P_q^{(1)}\}_{q=1}^{n_{\text{sel}}}$, where the superscript “(1)” is
 469 corresponding to $p_{\Theta}^{(1)}(\theta)$. Besides, the values of $h(\theta_q^{(1)}, t)$ and $p_X^{(1)}(x)$ for $q=1, \dots, n_{\text{sel}}$ are
 470 stored.

471 **Step 2.2.** If a perturbation of the source PDF is introduced, then $p_{\Theta}^{(1)}(\theta)$ will be
 472 correspondingly changed to $p_{\Theta}^{(2)}(\theta)$. Instead of conducting another complete round of PDEM
 473 analysis, the procedure of change of probability measure is implemented [26]. Accordingly, the
 474 new point set $M^{(2)} = \{\theta_q^{(1)}, P_q^{(2)}\}_{q=1}^{n_{\text{sel}}}$ is generated, where the point $\theta_q^{(1)}$ is unchanged, but the
 475 assigned probability is updated by $P_q^{(2)} = \int_{\Omega_q^{(1)}} p_{\Theta}^{(2)}(\theta) d\theta$, in which $\Omega_q^{(1)}$'s are the Voronoi cells.

476 **Step 2.3.** With the stored $h(\theta_q^{(1)}, t)$ and the updated assigned probability $P_q^{(2)}$, re-
 477 conduct **Steps 1.3** and **1.4** to obtain the updated PDF of output, $p_X^{(2)}(x)$.

478 Notice that the efficiency is improved by a factor of $\mathcal{O}(10^2) \sim \mathcal{O}(10^5)$ [26], which is
 479 mainly due to the reuse of the underlying deterministic analysis results in **Step 1.2**. It is
 480 noteworthy that, some similar but implied ideas can also be found, e.g., in [36] in the context
 481 of Bayesian updated PDEM, and in [37,38] in the context of Monte Carlo simulation, etc.

482

483 4.4. Approximation of Fréchet-Derivative-based GSI via PDEM-COM

484 By combining the PDEM and COM, the Fréchet-derivative-based GSI in Eq. (31) in a
 485 parametric form, can be evaluated by the following three steps:

486 **Step 3.1.** Estimate the original PDF $p_X(x)$. Notice that $p_X(x)$ is corresponding to
 487 $p_{\Theta}(\theta)$, where the embedded physical mechanism $X = g(\Theta)$ holds. From $p_{\Theta}(\theta)$ to $p_X(x)$,
 488 an uncertainty quantification method is needed. Traditionally, this part can be completed by,

489 e.g., the analytical method (for some simple cases) [35,39], the kernel density estimation (KDE)
 490 [40], or PDEM [28], etc. In the present paper, the PDEM outlined in Section 4.2 is adopted for
 491 its high accuracy and efficiency.

492 **Step 3.2.** Estimate the perturbed PDF $p_X^{(i)}(x)$ for $i = 1, \dots, n$. For the i -th input variable
 493 Θ_i , let a small perturbation be added on the PDF of Θ_i , i.e., p_{Θ_i} is changed to p'_{Θ_i} , and then
 494 the joint PDF becomes $p'_{\Theta}(\boldsymbol{\theta}) = \prod_{j=1, j \neq i}^n p_{\Theta_j}(\theta_j) \cdot p'_{\Theta_i}(\theta_i)$. Here the independence of basic
 495 random variables is assumed just for the sake of simplicity. If the input PDFs do not follow a
 496 specific model, but rather given by estimated histograms (data), the fourth-moment method
 497 could be an alternative, see Ref. [41] for details.

498 Further, assume this perturbation is only due to the change of distribution parameters of
 499 the input variables. For instance, if p_{Θ_i} can be uniquely determined by its first two moments,
 500 i.e., the mean value and standard deviation, denoted as $p_{\Theta_i}(\theta_i | \mu_i, \sigma_i)$, then this perturbation
 501 can be divided into two parts, namely, small variations of μ_i and σ_i , respectively. Then we
 502 have

$$503 \quad p'_{\Theta_i} = \begin{cases} p'_{\Theta_i|\mu_i}(\theta_i | \mu_i + \Delta\mu_i), \\ p'_{\Theta_i|\sigma_i}(\theta_i | \sigma_i + \Delta\sigma_i). \end{cases} \quad (53)$$

504 More generally, Eq. (53) can be written as [42]

$$505 \quad p_{\Theta|\Theta_i}^{(l)} = p_{\Theta|\Theta_i}^{(l)}(\boldsymbol{\theta} | \boldsymbol{\xi} + \mathbf{e}_{i,l} \Delta\xi_{i,l}), \quad i = 1, \dots, n; \quad l = 1, \dots, n_i \quad (54)$$

506 where $\mathbf{e}_{i,l}$ is a selection vector whose entries are zeros except its l -th location for the i -th
 507 variable being equal to one. The distribution parameters, denoted as $\boldsymbol{\xi}$, are perturbed by $\Delta\xi_{i,l}$
 508 and n_i is the total number of distribution parameters for the i -th random variable.

509 With the perturbed PDF $p_{\Theta|\Theta_i}^{(l)}$ in hand, the corresponding PDF of the response, see
 510 $p_X^{(i,l)}(x)$, should be computed. As discussed in [Section 4.3](#), in a recent paper by Chen & Wan
 511 [\[26\]](#), this time-consuming procedure can be greatly expedited by advocating the change of
 512 probability measure.

513 **Step 3.3.** Approximate the Fréchet derivative by the numerical difference scheme. From
 514 Eq. (31), the Fréchet derivative can be approximated by a forward difference scheme:

$$515 \quad \mathbb{F}_{\psi}^{(i,l)} \approx \frac{p_X^{(i,l)}(x) - p_X(x)}{\Delta \xi_{i,l}} \bigg/ \left\| \partial p_{\Theta} / \partial \xi_{i,l} \right\|_V, i = 1, \dots, n; l = 1, \dots, n_i \quad (55)$$

516 where the norm term is analytically calculated, see [Appendix B](#) in details.

517 Here the central difference scheme is suggested. To this end, a pair of perturbed PDF is in
 518 need, i.e., Eq. (54) is revised to

$$519 \quad \begin{cases} p_{\Theta|\Theta_i}^{(i,l)+} = p_{\Theta|\Theta_i}^{(i,l)}(\boldsymbol{\theta} | \boldsymbol{\xi} + \mathbf{e}_{i,l} \Delta \xi_{i,l}), \\ p_{\Theta|\Theta_i}^{(i,l)-} = p_{\Theta|\Theta_i}^{(i,l)}(\boldsymbol{\theta} | \boldsymbol{\xi} - \mathbf{e}_{i,l} \Delta \xi_{i,l}), \end{cases} i = 1, \dots, n, l = 1, \dots, n_i. \quad (56)$$

520 Besides, $p_X^{(i,l)+}$ and $p_X^{(i,l)-}$ are simultaneously generated by the PDEM-COM algorithm,
 521 respectively. Hence, Eq. (55) is modified by

$$522 \quad \mathbb{F}_{\psi}^{(i,l)} \approx \frac{1}{2} \frac{p_X^{(i,l)+}(x) - p_X^{(i,l)-}(x)}{\Delta \xi_{i,l}} \bigg/ \left\| \partial p_{\Theta} / \partial \xi_{i,l} \right\|_V, i = 1, \dots, n, l = 1, \dots, n_i. \quad (57)$$

523 Now we discuss the efficiency of the above algorithm. Denote the computational cost of
 524 evaluation of p_X for a certain p_{Θ} be C_0 . Let the total number of distribution parameters be
 525 $m = \sum_{i=1}^n n_i$ where n_i stands for the number of distribution parameters of the i -th random
 526 variable, then it is clear to see that, by the double-loop scheme, the total computational cost of
 527 sensitivity analysis would be $C_{D-L} = 2mC_0$ where the number 2 is due to the utilization of the
 528 central difference scheme. However, by the PDEM-COM algorithm the computational cost is
 529 $C_{\text{PDEM-COM}} = C_0 + 2mC_{\text{COM}}$, where C_{COM} is the computational cost for the calculation of

530 change of probability measure in **Step 2.2**. Since $C_{\text{COM}} \square C_0$, we have $C_{\text{PDEM-COM}} \approx C_0$.

531 Therefore, $\frac{C_{\text{D-L}}}{C_{\text{PDEM-COM}}} \approx 2m$, which indicates the high efficiency of the proposed PDEM-COM

532 scheme on evaluating the Fréchet-derivative-based GSI compared to the direct PDEM. Note

533 that compared to MCS and other methods, the efficiency of PDEM is again much higher by a

534 factor of $10 \sim 100$ or more. Therefore, the efficiency of evaluating the Fréchet-derivative-based

535 GSI by the PDEM-COM is higher than that of MCS by a factor of $20m \sim 200m$ or more.

536

537 **5 Numerical Applications**

538 To illustrate the Fréchet-derivative-based GSI and its numerical algorithm, five cases are

539 studied. Firstly, two analytical cases are investigated as benchmark tests. Then, three

540 engineering applications are exemplified.

541

542 *5.1. Example 1: The Riccati Equation*

543 We start with a simple case where only one random parameter is involved. A Riccati

544 equation with a random parameter is written as

$$545 \quad \dot{X}(t) + \Theta X^2(t) - X(t) = 0, \quad \dot{X} = dX / dt, \quad X(0) = 1 \quad (58)$$

546 where Θ is a random variable with the following log-normal PDF

$$547 \quad p_{\Theta}(\theta) = \frac{1}{\sqrt{2\pi}\sigma\theta} \exp\left\{-\frac{(\ln\theta - \mu)^2}{2\sigma^2}\right\} \quad (59)$$

548 where μ and σ are the distribution parameters. The analytical solution of Eq. (58) is [39]

$$549 \quad X = g(\Theta, t) = \frac{e^t}{\Theta e^t - \Theta + 1}. \quad (60)$$

550 Combining Eqs. (59) and (60), and according to the rule of change of random variable,

551 it is easy to obtain the PDF of X

552 $p_x(x,t) = \mathbf{J} \cdot p_\Theta(\theta = g^{-1}(x))$ (61)

553 where $\mathbf{J} = e^t / x^2 (e^t - 1)$ is the Jacobian. Expanding Eq. (61) yields

554
$$p_x(x,t) = \frac{1}{\sqrt{2\pi}x(e^t - x)\sigma} \exp \left\{ t - \frac{1}{2\sigma^2} \left\{ \ln \left(\frac{e^t - x}{xe^t - x} \right) - \mu \right\}^2 \right\}. \quad (62)$$

555 Notice that, all the known information characterizing the uncertainty, i.e., the PDF of Θ
 556 in Eq. (59), driven by the physical evolution mechanism by Eq. (60), is completely propagated
 557 into the PDF of QoI X , $p_x(x,t)$ in Eq. (62). Obviously, $p_x(x,t)$ is a functional of $p_\Theta(\theta)$,
 558 as explained in Eq. (2). Because $p_\Theta(\theta)$ is uniquely determined by μ and σ ; $p_x(x,t)$
 559 becomes a function of μ and σ , which is clearly exhibited in Eq. (62).

560

561 5.1.1. Analytical Solutions

562 Then, the Fréchet-derivative-based GSI can be obtained analytically by

563
$$\frac{\partial p_x}{\partial \mu} = \frac{1}{\sqrt{2\pi} (e^t - x) x \sigma^3} \exp \left\{ t - \frac{1}{2\sigma^2} \left(\ln \left\{ \frac{e^t - x}{xe^t - x} \right\} - \mu \right)^2 \right\} \left\{ \ln \left(\frac{e^t - x}{xe^t - x} \right) - \mu \right\} \quad (63)$$

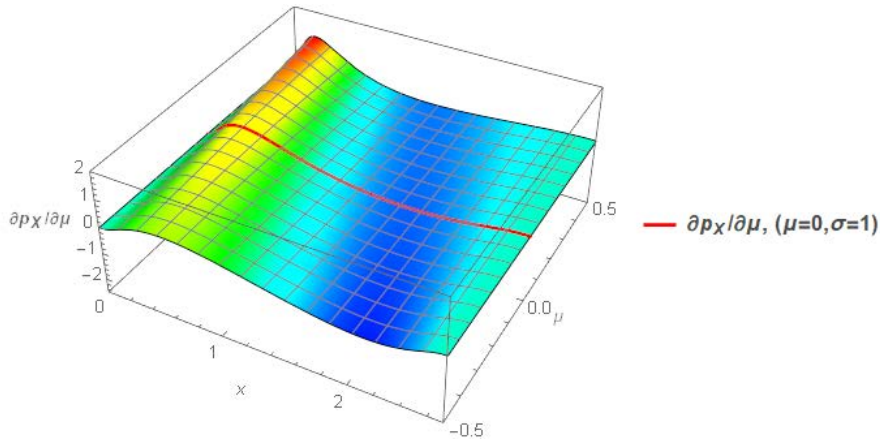
564 and

565
$$\begin{aligned} \frac{\partial p_x}{\partial \sigma} = & \frac{1}{\sqrt{2\pi} (e^t - x) x \sigma^4} \exp \left\{ t - \frac{1}{2\sigma^2} \left(\ln \left\{ \frac{e^t - x}{xe^t - x} \right\} - \mu \right)^2 \right\} \left\{ \ln \left(\frac{e^t - x}{xe^t - x} \right) - \mu \right\}^2 \\ & - \frac{1}{\sqrt{2\pi} (e^t - x) x \sigma^2} \exp \left\{ t - \frac{1}{2\sigma^2} \left(\ln \left\{ \frac{e^t - x}{xe^t - x} \right\} - \mu \right)^2 \right\} \end{aligned} \quad (64)$$

566 Here the norm terms with respect to the mean parameter is 0.3989 and the standard deviation
 567 parameter is 0.4839 (see [Appendix B](#)), and they are both omitted for simplicity without inducing
 568 confusion in [Section 5.1](#).

569 For clarity, we firstly study some properties of the Fréchet-derivative-based GSI from the
 570 analytical solutions. The numerical solutions by the PDEM-COM algorithm will be illustrated

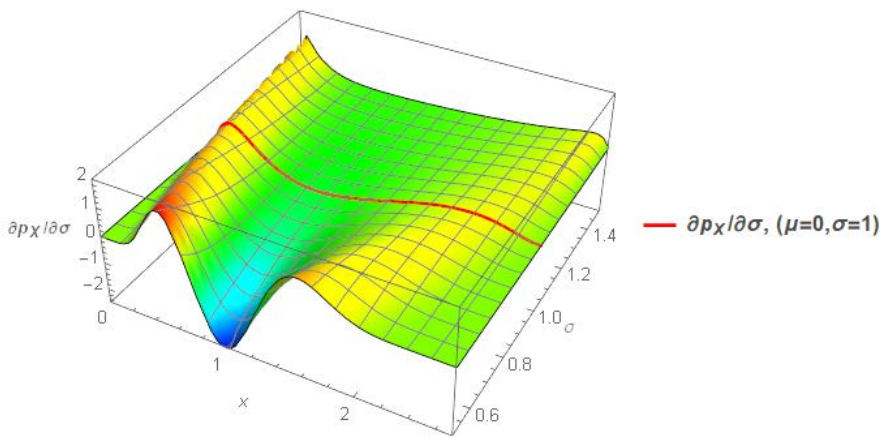
571 later in [Section 5.1.2](#). At a certain time instant $t = 1$, the conditional Fréchet derivative of Eq.
572 (63) in terms of μ with fixed $\sigma = 1$ is shown in [Fig. 1](#), while the conditional Fréchet
573 derivative of Eq. (64) in terms of σ when μ is fixed to 0 is shown in [Fig. 2](#). Several
574 observations can be made from these figures: (1) The Fréchet-derivative-based GSIs in terms
575 of the distribution parameters of basic random variables are curves rather than a single value,
576 which characterize the effects of change of the distribution parameters on the global, rather than
577 local properties of output QoI. (2) The Fréchet-derivative-based GSIs in terms of the
578 distribution parameters of basic random variables at different nominal values of the parameters
579 are quite different. For instance, from [Fig. 2](#) it is seen that the Fréchet-derivative-based GSI at
580 $\sigma = 1.4$ is much flatter than that at $\sigma = 0.6$, which implies that if the standard deviation of
581 source random variable is relatively small, then a slight perturbation of the input standard
582 deviation will induce relatively large perturbation on the PDF of output QoI. This is intuitively
583 reasonable; and (3) The surface of the Fréchet-derivative-based GSI in terms of σ looks more
584 complex than that in terms of μ . This means that generally the rule of influence of the standard
585 deviation of the basic random variable on QoI is more complex than that of the mean of the
586 basic random variable. Note that the change of mean of the basic random variable with fixed
587 standard deviation will make the source PDF shifted without shape changed, whereas the
588 change of standard deviation of the basic random variable with fixed mean value will make the
589 shape of source PDF changed. In other words, the complexity of change of source PDF induced
590 by the change of standard deviation is greater than that induced by the change of mean value of
591 the basic random variable. Therefore, the surface in [Fig. 2](#) being more complex than that in [Fig.](#)
592 [1](#) implies that if the change of source PDF is more complex, then the change of output PDF is
593 also more complex.



594

595

Fig. 1. Conditional Fréchet-derivative-based GSI with the change of μ ($\sigma = 1$).



596

597

Fig. 2. Conditional Fréchet-derivative-based GSI with the change of σ ($\mu = 0$).

598

599

600

601

602

603

604

To be clearer, consider the PDF of response $p_x(x, t)$ at $t = 1$ and its Fréchet-derivative-based GSIs at $\mu = 0$ and $\sigma = 1$. Then, the three curves by Eqs. (62) to (64) can be plotted in Fig. 3, respectively. A more vivid description of Fig. 3 is present in Fig. 4 in a vector form, where both the direction and rate of change of the value of PDF of output QoI due to the perturbation of input distribution parameters are shown. From these figures, it can be observed that:

605

606

607

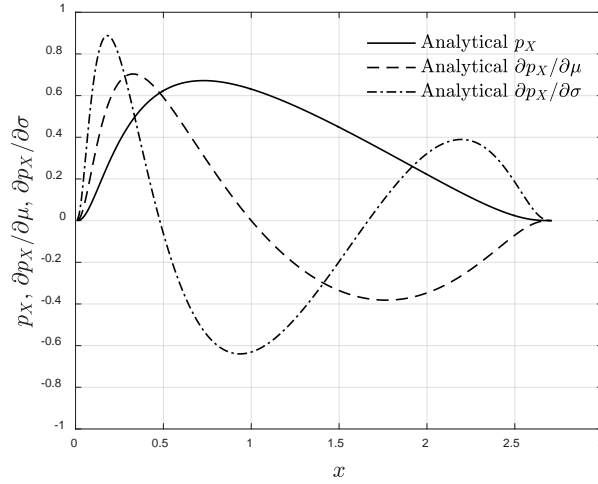
608

Firstly, it is noticed from Fig. 3 that the curves of Fréchet-derivative-based GSIs are not always positive or negative, nor are they monotonic functions. Actually, by inspection it is seen that there is at least one intermediate point crossing the abscissa besides the left and right ends of the curve, and the area between the curves of Fréchet-derivative-based GSIs and the abscissa

609 is zero, which is consistent with Eq. (43). It is seen that at the left and right tails of PDF of the
610 output QoI, the values of Fréchet-derivative-based GSIs are close to zero. Besides, there is one
611 single intermediate point at the curve of Fréchet-derivative-based GSI in terms of the mean of
612 source random variable crossing the abscissa, whereas there are two intermediate points at the
613 curve of Fréchet-derivative-based GSI in terms of the standard deviation of source random
614 variable crossing the abscissa. This is also noticed in the preceding paragraph that the surface
615 in Fig. 2 is more complex than that in Fig. 1.

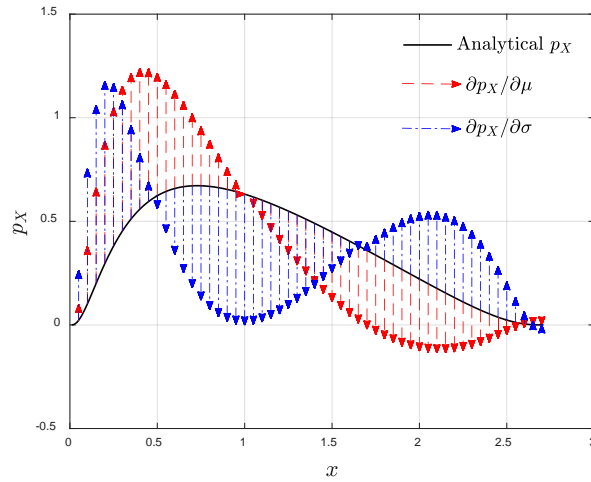
616 Secondly, in Fig. 4 it is shown how the PDF of the output QoI will change if there is
617 perturbation in the distribution parameters of the source random variable. It is seen that, if the
618 mean of the source random variable increases, then the left part of PDF of the output QoI will
619 increase (according to the direction of the arrows) and the right part will decrease, resulting in
620 a PDF of the output QoI with centroid (the mean value of output QoI) shifted to left. On the
621 other hand, if the standard deviation of the source random variable increases, then the left and
622 right part of the PDF of output QoI will increase and the middle part will decrease, which means
623 that the PDF of output QoI will become flatter. This also implies that the standard deviation of
624 the output QoI will increase. Quantitatively, the change of PDF of the output QoI due to the
625 perturbation of mean of the source random variable in the neighborhoods of 0.4 and 1.6 (in the
626 response space) is much greater than that in other areas (see Fig. 3), whereas the change of PDF
627 of the output QoI due to the perturbation of standard deviation of the source random variable
628 in the neighborhoods of 0.2, 0.9 and 2.2 (the extrema of the curve in Fig. 3) is much greater
629 than that in other areas. This information is of course useful for decision-making for practical
630 engineering problems, because the quantitative effects on the possible subset in the response
631 space due to perturbation of mean and standard deviation of source random variable are
632 captured.

633 The above discussions demonstrate that, different from most existent GSI indices, the
 634 Fréchet-derivative-based GSI can not only reflect how much the sensitivity is in a global sense
 635 via the change of PDF of output QoI, but also point out the certain direction of such change.
 636



637
 638 **Fig. 3.** PDF of QoI at $t = 1$ and its Fréchet-derivative-based GSI ($\mu = 0$ and $\sigma = 1$).

639



640
 641 **Fig. 4.** PDF of QoI at $t = 1$ and its Fréchet-derivative-based GSI in vector form ($\mu = 0$ and $\sigma = 1$).

642

643 **Remark 2.1:** Specifically, if the failure domain is defined as $\Omega_f : X < x_{lim}$, by integrating

644 Eqs. (63) and (64) we have

$$645 \quad \int_{\Omega_f} \frac{\partial p_x}{\partial \mu} dx = \frac{\partial P_f}{\partial \mu} \Big|_{x=x_{\text{lim}}} , \quad \int_{\Omega_f} \frac{\partial p_x}{\partial \sigma} dx = \frac{\partial P_f}{\partial \sigma} \Big|_{x=x_{\text{lim}}} . \quad (65)$$

646 Eq. (65) is exactly the sensitivity of failure probability with respect to the distribution
647 parameters of input random variables, see also related researches in [4,42-43].

648 The analytical expressions of Eq. (65) is

$$649 \quad \frac{\partial P_f}{\partial \mu} = -\frac{1}{\sqrt{2\pi}\sigma} \exp \left\{ -\frac{1}{2\sigma^2} \left(\ln \left\{ \frac{e^t - x}{xe^t - x} \right\} - \mu \right)^2 \right\} \Big|_{x=x_{\text{lim}}} \quad (66)$$

650 and

$$651 \quad \frac{\partial P_f}{\partial \sigma} = -\frac{1}{\sqrt{2\pi}\sigma^2} \exp \left\{ -\frac{1}{2\sigma^2} \left(\ln \left\{ \frac{e^t - x}{xe^t - x} \right\} - \mu \right)^2 \right\} \cdot \left(\mu - \ln \left\{ \frac{e^t - x}{xe^t - x} \right\} \right) \Big|_{x=x_{\text{lim}}} . \quad (67)$$

652 Meanwhile, the analytical expression of failure probability P_f is given by

$$653 \quad P_f = \int_{-\infty}^{x_{\text{lim}}} p_x dx = 1 - \frac{1}{2} \operatorname{erf} \left\{ \frac{1}{\sqrt{2}\sigma} \left(\mu - \ln \left\{ \frac{e^t - x}{xe^t - x} \right\} \right) \right\} \Big|_{-\infty}^{x_{\text{lim}}} \quad (68)$$

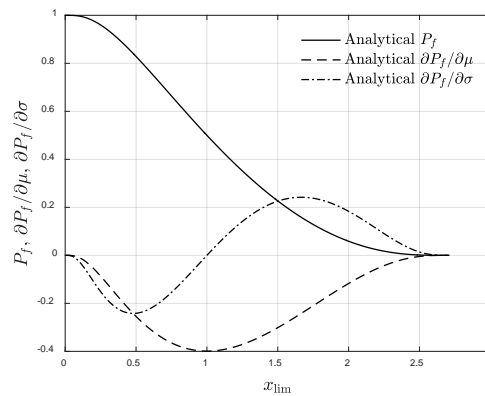
654 where $\operatorname{erf}(\cdot)$ is the Gaussian error function.

655 It should be emphasized that, similar but unlike the researches in [4,42], the present paper
656 aims to propose a new GSI with respect to the PDF of output QoI, rather than the failure
657 probability of QoI. But the sensitivity of failure probability of QoI can be a byproduct of the
658 proposed GSI, as shown in Eqs. (6) and (65). Moreover, the proposed GSI in the present paper
659 can be evaluated efficiently by the PDEM-COM method, which makes it more applicable for
660 practical applications.

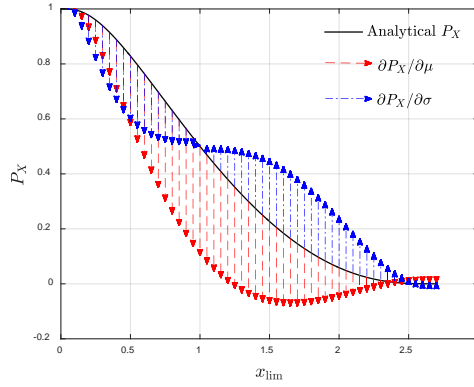
661 **Remark 2.2:** Similarly, Eqs. (66) to (68) are plotted in Figs. 5 and 6 to gain a more
662 straightforward and intuitive understanding on how P_f is sensitive to the input variable. At
663 first glance it is noticed that the sensitivity of P_f at the end points of x_{lim} is zero. This is

664 reasonable because $\lim_{x_{\text{lim}} \rightarrow -\infty} P_f = 1$ and $\lim_{x_{\text{lim}} \rightarrow \infty} P_f = 0$, i.e., the failure probability will not change

665 against the change of mean and standard deviation of source random variable at these two
666 extreme points. In addition, different from the sensitivity curves in Fig. 3, the sensitivity curves
667 in Fig. 5 can be always positive or always negative, or partly positive but partly negative.
668 Interestingly, it is shown that a positive perturbation of μ will always reduce P_f of QoI, see
669 the direction of the arrows in Fig. 6, and compare the curves with and without perturbation of
670 the mean of source random variable in Fig. 7. On the other hand, as σ increases, there are
671 different situations in two intervals: for $x_{\text{lim}} \in (-\infty, 1)$, P_f will decrease; while for
672 $x_{\text{lim}} \in (1, +\infty)$, P_f will increase, see the direction of the arrows in Fig. 6, and compare the
673 curves with and without perturbation of the standard deviation of source random variable in Fig.
674 8. Therefore, there is a crucial point, i.e., $x_{\text{lim}} = 1$, which makes P_f of QoI stays insensitive
675 to the input variable, at least for the distribution parameter of σ . Again, here it is noticed that
676 the effect of perturbation of the standard deviation of source random variable on the failure
677 probability is more complex than that of the mean of source random variable. Evidently, for
678 engineering purposes, the above analytical results will provide valuably qualitative and
679 quantitative information for designers and decision-makers.

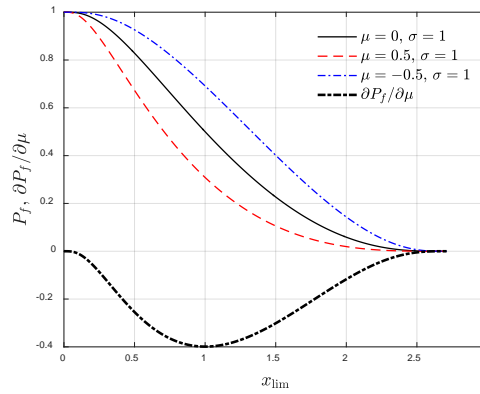


680
681 **Fig. 5.** Failure probability of QoI and its Fréchet-derivative-based GSI ($\mu = 0$, $\sigma = 1$ and $t = 1$).



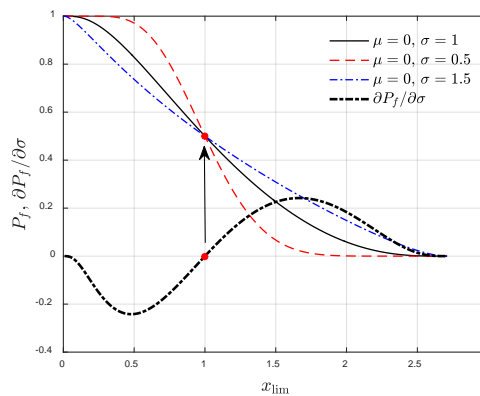
682

683 **Fig. 6.** Failure probability of QoI and its Fréchet-derivative-based GSI in vector form ($\mu = 0$, $\sigma = 1$
 684 and $t = 1$).



685

686 **Fig. 7.** The influence of μ on failure probability ($\sigma = 1$ and $t = 1$).



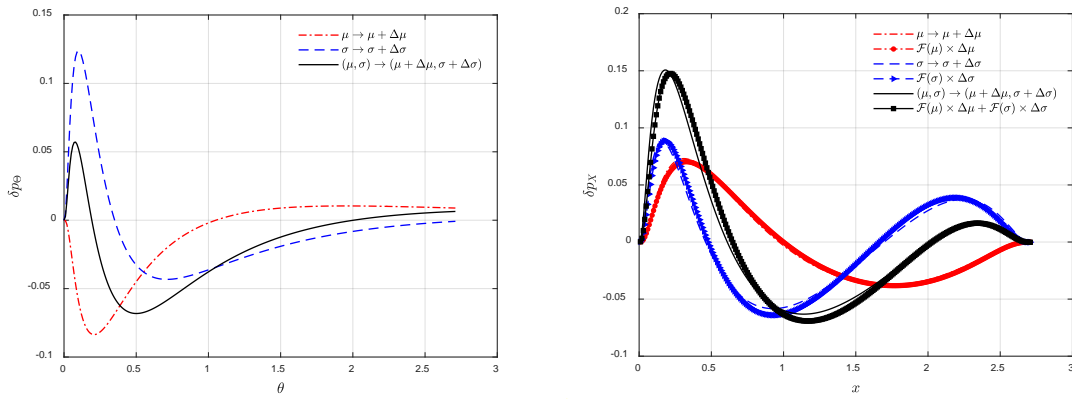
687

688 **Fig. 8.** The influence of σ on failure probability ($\mu = 0$ and $t = 1$).

689

690 **Remark 2.3:** The proposed Fréchet-derivative-based GSI can be naturally utilized to
 691 observe the variation of the output PDF of QoI, when the input PDF gives some variations. In

692 Fig.9, assume the input PDF is perturbed in three ways: (1) the parameter μ is changed from
693 0 to 0.1, (2) the parameter σ is set from 1 to 1.1 and (3) the parameters (μ, σ) are chosen
694 from (0,1) to (0.1,1.1), i.e., to be changed simultaneously. Then the proposed GSI presented in
695 Eqs. (63) and (64) are taken into calculation, where one can see that a good linear
696 approximation is achieved, compared with analytical results. It should be emphasized again that
697 though the proposed GSI is under a framework of parametric distributions, it serves well to
698 observe the variation of output PDF when the input PDF is changed, see the third case in Fig.
699 9 when both parameters are perturbed.



700
701 (a) The variation of input PDF (b) The variation of output PDF via analysis and proposed
702 GSI

703 **Fig. 9.** A direct function of the proposed Fréchet-derivative-based GSI.

704
705 5.1.2. Numerical Solutions by the PDEM-COM Method

706 To numerically evaluate the Fréchet-derivative-based GSIs, one round of PDEM analysis
707 is firstly required. To this end, 100 representative points are firstly generated by the GF-
708 discrepancy minimized strategy [31], and then an ensemble evolution scheme of PDEM [44] is
709 adopted to evaluate the PDF of output QoI, $p_X(x; \mu, \sigma)$. Next, without additional evaluations
710 of the Riccati equation, the COM is implemented to estimate the four perturbed PDFs of QoI
711 [26], namely $p_X(x; \mu + \Delta\mu, \sigma)$, $p_X(x; \mu - \Delta\mu, \sigma)$, $p_X(x; \mu, \sigma + \Delta\sigma)$ and

712 $p_X(x; \mu, \sigma - \Delta\sigma)$, respectively. By the central difference scheme, the Fréchet-derivative-based

713 GSI are then approximated by

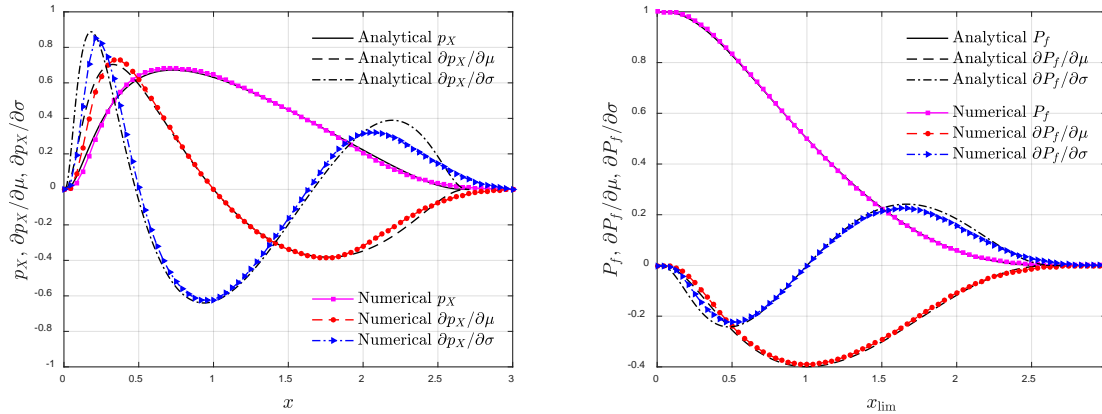
$$714 \frac{\partial p_X}{\partial \mu} \approx \frac{\Delta p_X}{\Delta \mu} = \frac{1}{2} \frac{p_X(x; \mu + \Delta\mu, \sigma) - p_X(x; \mu - \Delta\mu, \sigma)}{\Delta \mu} \quad (69)$$

715 and

$$716 \frac{\partial p_X}{\partial \sigma} \approx \frac{\Delta p_X}{\Delta \sigma} = \frac{1}{2} \frac{p_X(x; \mu, \sigma + \Delta\sigma) - p_X(x; \mu, \sigma - \Delta\sigma)}{\Delta \sigma} \quad (70)$$

717 respectively, where $\Delta\mu$ and $\Delta\sigma$ take small values, say 0.1 in this case.

718 Shown in Fig. 10 is the comparison between the analytical solutions and the numerical
 719 solutions by PDEM-COM, which demonstrates a good accuracy of the proposed method. In
 720 spite of some errors between analytical solutions and numerical ones in Fig. 10(a), the major
 721 shape and magnitude are consistent. Meanwhile, as for the sensitivity of failure probability of
 722 QoI in Fig. 10(b), the error is relatively small.



723 (a) Sensitivity of PDF of QoI

724 (b) Sensitivity of CDF (failure probability) of QoI

725 **Fig. 10.** Comparison between analytical solutions and numerical solutions via PDEM-COM.

726

727 5.2. Example 2: Sum of Gaussian Random Variables

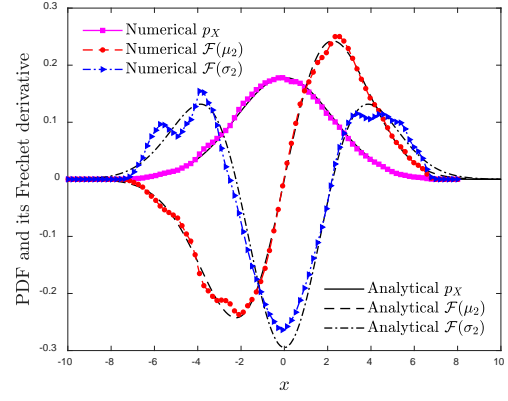
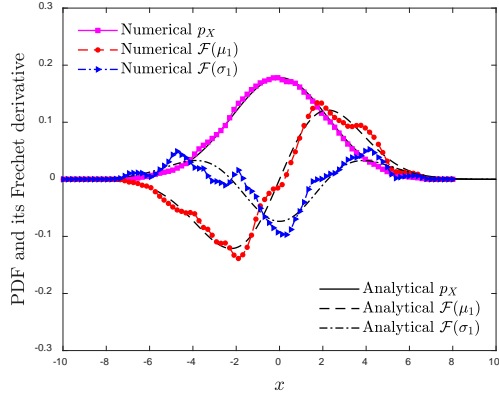
728 5.2.1. Subcase 1

729 Consider two independent random variables Θ_1 and Θ_2 , and the QoI X is given by
 730 the following function:

731 $X = \Theta_1 + 2\Theta_2.$ (71)

732 Assume both Θ_1 and Θ_2 are normally distributed random variables with mean values
733 μ_1 and μ_2 , and standard deviations σ_1 and σ_2 , respectively. To avoid lengthiness here, the
734 analytical expressions of the Fréchet-derivative-based GSI in terms of μ_1 , μ_2 , σ_1 and σ_2
735 are provided in [Appendix C](#).

736 Without loss of generality, assume $\mu_1 = \mu_2 = 0$ and $\sigma_1 = \sigma_2 = 1$. The numerical results
737 are shown in [Figs. 11 and 12](#), compared with the analytical solutions in [Appendix C](#). In this
738 case, a fairly good approximation is achieved in [Fig. 11](#), while a perfect agreement is observed
739 in [Fig. 12](#) as well. With all these informative results at hand, some valuable conclusions can be
740 drawn here: (1) Obviously, it is easy to find that in this system the PDF of output QoI is more
741 sensitive to Θ_2 than to Θ_1 because the maximum value of the GSIs in terms of parameters
742 of Θ_2 in [Fig. 11\(b\)](#) are greater by twice than the corresponding ones of Θ_1 in [Fig. 11\(a\)](#),
743 which is intuitively reasonable from Eq. (71); (2) Similar to Example 1, in each sensitivity
744 curve in terms of the mean of source random variables only one single intermediate point
745 crossing the abscissa exists in [Fig. 11\(a\)](#), whereas in each sensitivity curve in terms of the
746 standard deviation of source random variables there are two intermediate points crossing the
747 abscissa in [Fig. 11\(b\)](#); and (3) The failure probability will certainly always increase due to a
748 small increment of the mean values as shown in [Fig. 12](#), while for the standard deviations, the
749 influence of increasing or reducing the failure probability is dependent on the threshold.
750 Interestingly, similar to Example 1, there also exists a fixed point at $x_{\text{lim}} = 0$.



751

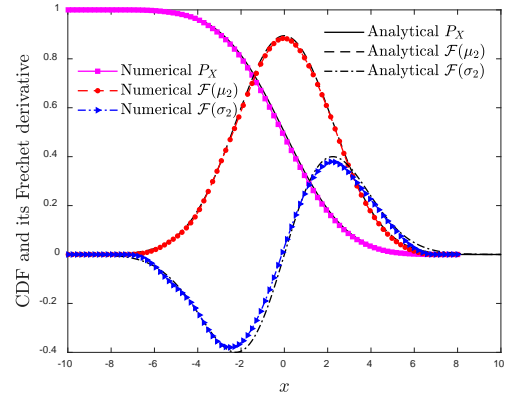
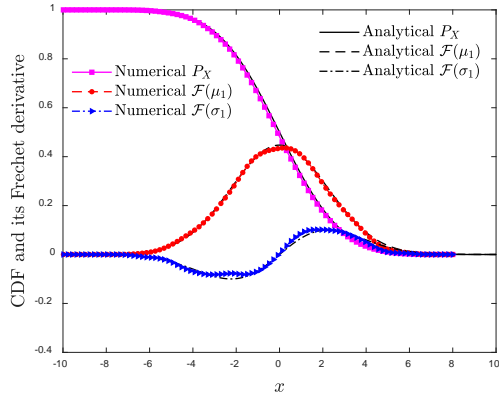
752

(a) Sensitivity of PDF of QoI for Θ_1

(b) Sensitivity of PDF of QoI for Θ_2

753

Fig. 11. Fréchet-derivative-based GSIs of PDF in terms of Θ_1 and Θ_2 .



754

755

(a) Sensitivity of failure probability of QoI for Θ_1

(b) Sensitivity of failure probability of QoI for Θ_2

756

Fig. 12. Fréchet-derivative-based GSI of failure probability in terms of Θ_1 and Θ_2 .

757

758 5.2.2. Subcase 2

759

Now we consider two similar but not identical functions:

760

$$(a) X_a = \Theta_1 + \Theta_2 \quad \text{and} \quad (b) X_b = \Theta_1 - \Theta_2 \quad (72)$$

761

where the subscripts “a” and “b” denote the QoIs that generated by Eqs. (72)a and (72)b, or

762

Subcase 2a and Subcase 2b, respectively. The information of Θ_1 and Θ_2 is identical to that

763

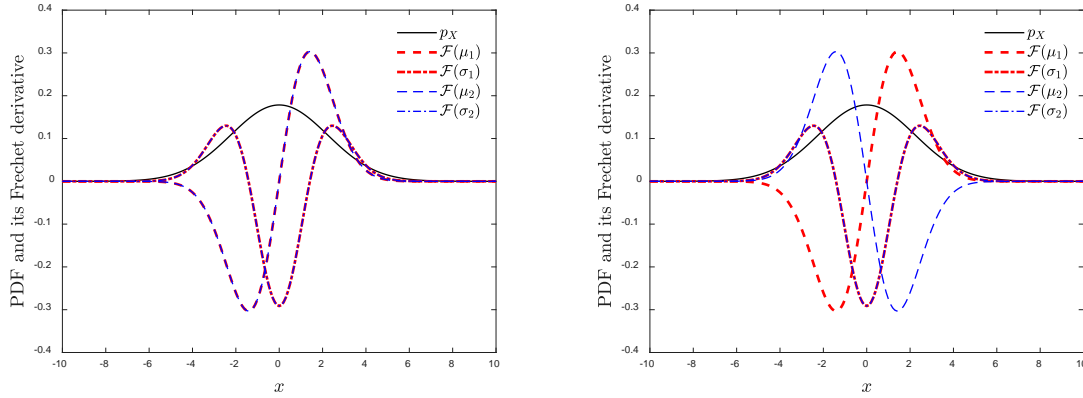
in Subcase 1. Therefore, X_a and X_b are normally distributed as well. To avoid lengthiness

764

here, the analytical expressions of Fréchet-derivative-based GSI of X_a and X_b are available

765 in [Appendix C](#). Again, let $\mu_1 = \mu_2 = 0$ and $\sigma_1 = \sigma_2 = 1$. The Fréchet-derivative-based GSIs
 766 for Subcase 2a and Subcase 2b are shown in [Fig. 13](#).

767



768

769 (a) Fréchet-derivative-based GSIs for Subcase 2a (b) Fréchet-derivative-based GSIs for Subcase 2b

770

Fig. 13. Fréchet-derivative-based GSIs for two Subcases.

771

772 From [Fig. 13](#), it is easy to observe how each input variable affects the QoI in terms of both
 773 magnitude and direction. It is clearly seen that the proposed GSIs in Subcase 2a are apparently
 774 different from those in Subcase 2b. Actually, from [Fig. 13\(a\)](#) it is seen that the sensitivity curves
 775 in terms of the means of both source variables are identical. Simultaneously, the sensitivity
 776 curves in terms of the standard deviations of both source variables are also identical. This is
 777 intuitively reasonable because from [Eq. \(72\)a](#) it is noticed that the QoI is symmetric in terms of
 778 Θ_1 and Θ_2 . However, from [Fig. 13\(b\)](#) it is noticed that, though the sensitivity curves in terms
 779 of the standard deviations of both source variables are still identical, the sensitivity curves in
 780 terms of the means of the two source random variables are not identical any more. Actually, in
 781 this case, the amplitudes are still identical but the signs are opposite. Considering the QoI in [Eq.](#)
 782 [\(72\)b](#) is anti-symmetric in terms of Θ_1 and Θ_2 , again the properties shown in [Fig. 13\(b\)](#) are
 783 intuitively understandable.

784 Unfortunately, the existent sensitivity indices, including the Sobol' indices [13] or
 785 moment-independent importance measures [16] as listed in Table 2, cannot distinguish the
 786 sensitivity of Θ_1 and Θ_2 in Eq. (72)b. It is seen from Table 2 that there is no difference
 787 between the sensitivity indices of Subcase 2a and Subcase 2b, which is somewhat misleading
 788 [17].

789

790 **Table 2**

791 Analytical results of Subcase 2a and Subcase 2b [17].

Subcases	Subcase 2a		Subcase 2b	
Input variables	Θ_1	Θ_2	Θ_1	Θ_2
Sobol' indices:	0.5	0.5	0.5	0.5
Moment-independent IMs:	0.306	0.306	0.306	0.306

792

793 5.3. Example 3: A Cantilever Beam

794 In this case, a cantilever beam subjected to two concentrated forces is studied [45], as
 795 shown in Fig. 14. The responses of the beam, i.e., the maximum displacement and stress, can
 796 be analytically obtained, thus we have the following two performance functions:

797 (a) displacement performance function

$$798 \quad g_D = d_0 - \frac{4L^3}{Ewh} \sqrt{\left(\frac{Y}{h^2}\right)^2 + \left(\frac{X}{w^2}\right)^2}, \quad (73)$$

799 (b) stress performance function

$$800 \quad g_S = R - \frac{6L}{wh^2}(X + Y) \quad (74)$$

801 where all the parameters in Eqs. (73) and (74) are listed in Table 3.

802

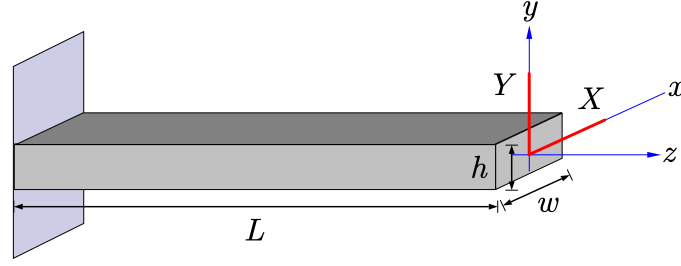


Fig. 14. A cantilever beam structure [45].

803

804

805

806

807

808

809

810

811

812 **Table 3**

813 Model parameters in the cantilever beam structure.

Parameters	Value/Distribution	Mean	Std.D	Physical senses
L (in)	100	-	-	Beam length
w (in)	4	-	-	Beam width
h (in)	2	-	-	Beam thickness
d_0 (in)	5	-	-	Displacement threshold
X (lbf)	Normal	500	100	Horizontal force
Y (lbf)	Normal	1000	100	Vertical force
E (psi)	Normal	2.9×10^7	1.45×10^6	Modulus of elasticity
R (psi)	Normal	6.4×10^4	3.2×10^4	Yield stress

814

815 In this practical case, it is emphasized that since the unit of each parameter is different,
816 thus the digital values of realizations of different random variables may differ for several orders
817 of magnitude. For instance, the order of magnitude of vertical force is about $\mathcal{O}(10^3)$ while
818 the order of magnitude of the modulus of elasticity is around $\mathcal{O}(10^7)$. This of course may
819 induce numerical singularity. Therefore, in this aspect, the norm term in the proposed Fréchet-
820 derivative-based GSI in Eq. (31) can be regarded as a non-dimensional-normalization factor,
821 which is naturally defined in the definition of the Fréchet derivative, i.e.,

$$822 \left\{ \begin{array}{l} \frac{\partial p / \partial \mu_X}{\|\partial p_\Theta / \partial \mu_X\|}, \frac{\partial p / \partial \mu_Y}{\|\partial p_\Theta / \partial \mu_Y\|}, \frac{\partial p / \partial \mu_E}{\|\partial p_\Theta / \partial \mu_E\|}, \frac{\partial p / \partial \mu_R}{\|\partial p_\Theta / \partial \mu_R\|}, \\ \frac{\partial p / \partial \sigma_X}{\|\partial p_\Theta / \partial \sigma_X\|}, \frac{\partial p / \partial \sigma_Y}{\|\partial p_\Theta / \partial \sigma_Y\|}, \frac{\partial p / \partial \sigma_E}{\|\partial p_\Theta / \partial \sigma_E\|}, \frac{\partial p / \partial \sigma_R}{\|\partial p_\Theta / \partial \sigma_R\|}. \end{array} \right. \quad (75)$$

823 where p stands for the PDF of QoI, i.e., the displacement performance function g_D , or the
824 stress performance function g_S , while p_Θ denotes the PDF of inputs.

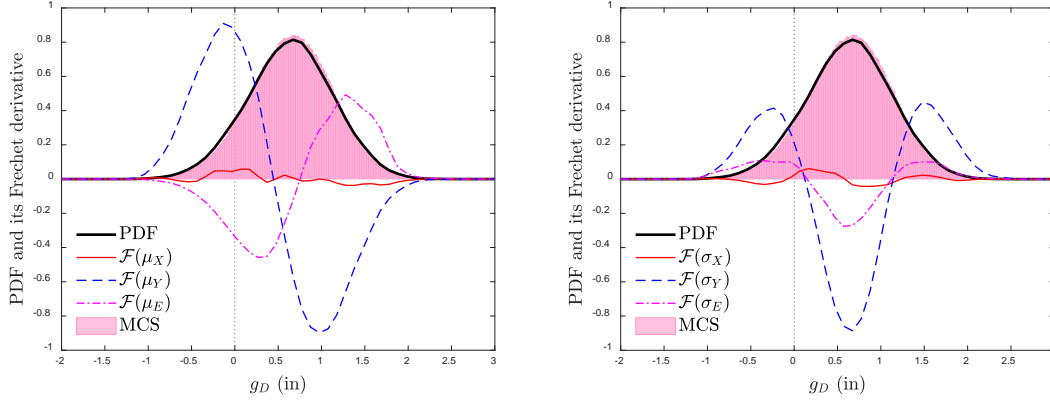
825

826 5.3.1. The GSI of the Displacement Performance Function

827 Let the QoI firstly be g_D . Numerical results of the GSI by the PDEM-COM method are
828 plotted in Fig. 15. By inspection some instructive properties are clear: (1) For the mean values
829 of distribution parameters of the source random variables, μ_Y is of most influence, while the
830 effect of μ_X is comparatively very small. Noting from Table 3 that w is twice h from Eq. (73)
831 so it can be estimated roughly that the effect of Y should be at least greater than that of X by a
832 factor of around $(2)^2 = 4$. This is consistent with the above observation. (2) Moreover, it is noted
833 that the GSIs of QoI in terms of μ_Y and μ_E are almost completely opposite in Fig. 15(a),
834 which is also reasonable since Y is related to the external load effect, while E stands for the
835 intrinsic structural resistance. From a physical perspective, the effects of these two variables
836 must be opposite. And (3) it is seen that, in terms of Y and E , the mean values of source random

837 variables have greater effects on QoI than the standard deviations of source random variables
 838 by comparing Figs. 15(a) and 15(b).

839



840

841 (a) GSI with respect to the mean value (b) GSI with respect to the standard deviation

841

842 **Fig. 15.** PDF of g_D and its Fréchet-derivative-based GSIs.

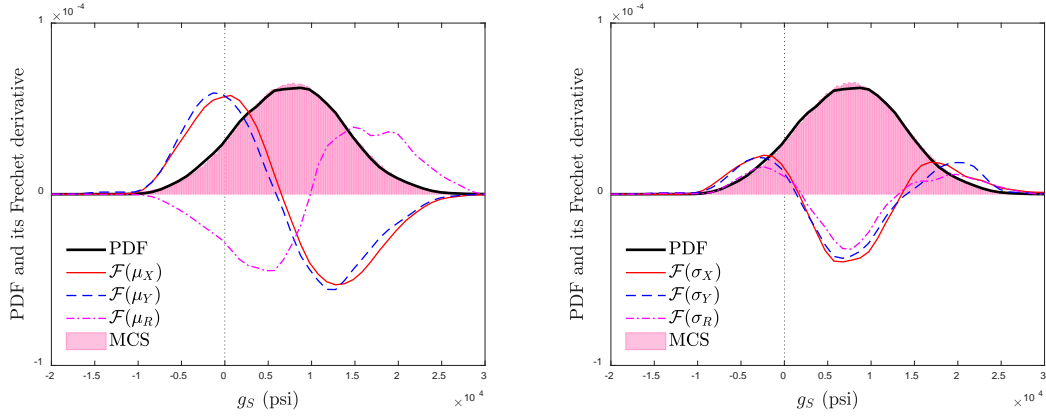
842

843

844 **5.3.2. Stress Performance Function**

845 Now we consider g_S . The GSIs are plotted in Fig. 16. It is clear to see that: (1) μ_X , μ_Y
 846 and μ_R are all of remarkable effect on QoI, in an order of $\mu_Y \approx \mu_X > \mu_R$ in terms of
 847 sensitivity, which is easily understandable from Eq. (74). In particular, in this case because X
 848 has the same factor -1 as that of Y from Eq. (74), it is roughly estimated that the sensitivity of
 849 X is close to that of Y , which is verified from Fig. 16(a). This is also true for the μ_R but
 850 because the factor of R becomes to 1 so the direction of GSI based on μ_R is opposite to those
 851 of μ_X and μ_Y . (2) Besides, σ_X , σ_Y and σ_R are of less and close effect, which is due to
 852 the coincidence that $\sigma_R = 3200\text{psi}$ while $\frac{6L}{wh^2}\sigma_X = \frac{6L}{wh^2}\sigma_Y = 3750\text{psi}$ from Eq. (74), but
 853 one can still see that the effects of σ_X , σ_Y and σ_R are in an order of $\sigma_Y \approx \sigma_X > \sigma_R$.

854



855

856

(a) GSI with respect to the mean value (b) GSI with respect to the standard deviation

857

Fig. 16. PDF of g_S and its Fréchet-derivative-based GSIs.

858

859 5.3.3. Discussion and Verification

860

861

862

863

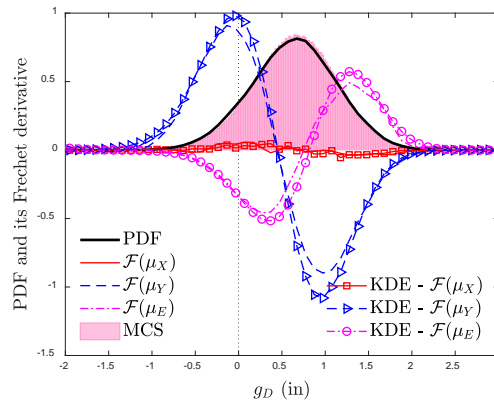
864

865

866

867

Actually, since it is not always easy to obtain the analytical expressions of Example 3, the results by the Monte Carlo Simulation (MCS) are adopted as a reference. The kernel density estimation (KDE) [40], as an important method in sensitivity analysis, is employed to estimate the probability density function. One million times of evaluations are completed for one single loop of sensitivity analysis, and the results are shown in Fig. 17. Compared with the numerical results plotted in Fig. 15(a), the accuracy of the GSIs by PDEM-COM is again verified, but the efficiency of PDEM-COM is much higher since only 500 function evaluations are needed for the whole analysis.



868

869

Fig. 17. Comparison between PDEM-COM and MCS-KDE.

870

871 *5.4. Example 4: The Short Column Function*

872 The short column function is commonly utilized as a benchmark in reliability-based
873 structural optimization [45-47]. The limit state function is explicitly defined as

874
$$g(M_1, M_2, P, Y) = 1 - \frac{4M_1}{bh^2Y} - \frac{4M_2}{b^2hY} - \left(\frac{P}{bhY}\right)^2 \tag{76}$$

875 where Y stands for the yield stress, b and h are the width and depth of the rectangular
876 cross section of the short column, which is subjected to bi-axial bending moments M_1 and
877 M_2 . According to [46], the geometrical parameters b and h are all set to the optimal values,
878 e.g., 300mm and 600mm, respectively. The uncertainty is considered to be originated from M_1 ,
879 M_2 , P and Y with the probability distributions listed in Table 4. Here the statistically
880 independency of M_1 , M_2 , P and Y is assumed for simplicity.

881

882 **Table 4**

883 Model parameters in the short column function [46].

Parameters	Distribution	Mean	C.O.V.	Physical senses
M_1 (kN · m)	Lognormal	250	0.30	Bending moment
M_2 (kN · m)	Lognormal	125	0.30	Bending moment
P (kN)	Weibull	2500	0.20	Axial force
Y (MPa)	Gamma	40	0.10	Yield stress

884 Note: C.O.V. is the abbreviation of coefficient of variation.

885

886 The first and second distribution parameters of M_1 , M_2 , P and Y are analytically
887 calculated by the mean value and the standard deviation listed in Table 4, and are denoted by

888 (a_{M_1}, b_{M_1}) , (a_{M_2}, b_{M_2}) , (a_P, b_P) and (a_Y, b_Y) , respectively. Specifically, the PDFs of M_1 ,
 889 M_2 , P and Y are correspondingly written by

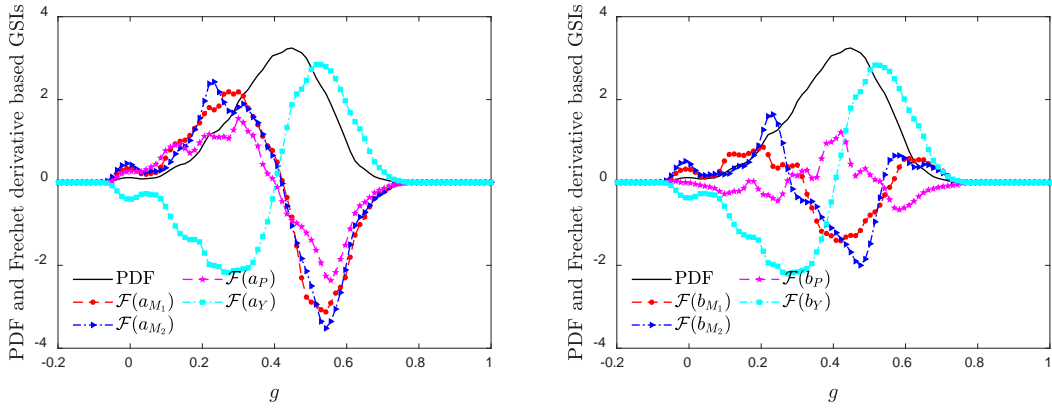
$$\begin{cases}
 p_{M_1}(x; a_{M_1}, b_{M_1}) = \frac{1}{x\sqrt{2\pi}b_{M_1}} \exp\left\{-\frac{(\ln x - a_{M_1})^2}{2b_{M_1}^2}\right\}, \\
 p_{M_2}(x; a_{M_2}, b_{M_2}) = \frac{1}{x\sqrt{2\pi}b_{M_2}} \exp\left\{-\frac{(\ln x - a_{M_2})^2}{2b_{M_2}^2}\right\}, \\
 p_P(x; a_P, b_P) = \frac{b_P}{a_P} \left(\frac{x}{a_P}\right)^{b_P-1} \exp\left\{-\left(\frac{x}{a_P}\right)^{b_P}\right\}, \\
 p_Y(x; a_Y, b_Y) = \frac{1}{b_Y^{a_Y} \Gamma(a_Y)} x^{a_Y-1} \exp\left(-\frac{x}{b_Y}\right)
 \end{cases} \quad (77)$$

891 where $\Gamma(\cdot)$ is the Gamma function.

892 The Fréchet-derivative-based GSIs evaluated by the PDEM-COM method are plotted in
 893 Fig. 18. It is seen from Fig. 18 that the GSIs in terms of the first and second parameters of M_1
 894 are almost identical to those in terms of M_2 , respectively. This is actually the reflection of the
 895 fact from Eq. (76) that the function is symmetric in terms of M_1 and M_2 . Moreover, it can be
 896 seen clearly that the influence of the first parameter of Y on PDF of g is in an opposite way
 897 compared to the effects of the means of M_1 , M_2 and P . This can be easily interpreted:
 898 according to Eq. (76), Y is in the dominator while M_1 , M_2 and P are all in the numerator.
 899 In the reliability-based structural optimization, the direction (sign) of sensitivity in terms of
 900 basic input variables is of paramount significance [48]. A verification of the proposed PDEM-
 901 COM is also completed in Fig. 19 via the MCS-KDE as illustrated in Example 3. Here we
 902 arbitrarily verify some of the indices in Fig. 18, and the verified results in Fig. 19 indicate a
 903 high accuracy of the proposed method of calculating the proposed GSI.

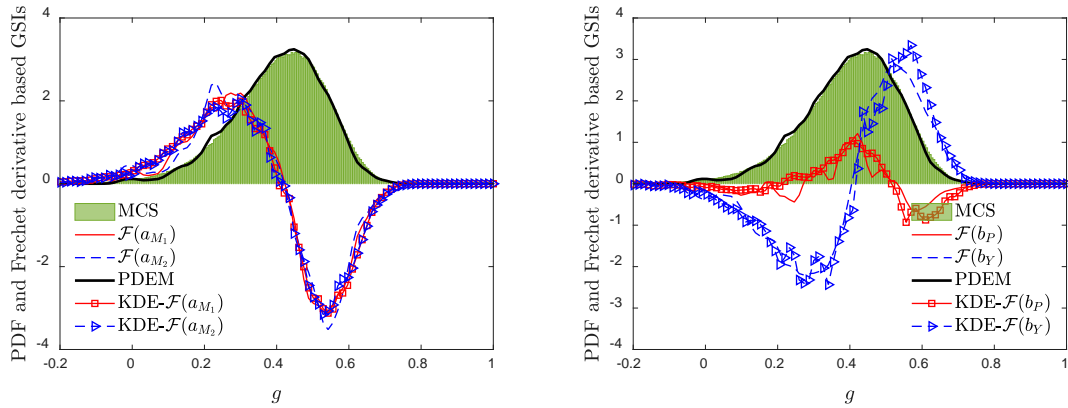
904 In a sense, this kind of opposite or positive influences (direction) on the PDF of QoI, are
 905 natural sensitivities with certain directions due to the embedded physical mechanisms, which

906 can be captured by the proposed Fréchet-derivative-based GSIs.



907
908 (a) GSI with respect to the first parameter (b) GSI with respect to the second parameter

909 **Fig. 18.** Fréchet-derivative-based GSIs in terms of the first and second parameters in Example 4.



910
911 **Fig. 19.** Fréchet-derivative-based GSIs in terms of the first and second parameters in Example 4 via
912 PDEM-COM and MCS-KDE.

914 **5.5. Example 5: A Roof Truss Structure**

915 A more complex case involving a roof truss structure [6] is studied hereinafter (Fig. 20).
916 The structure is subjected to uniformly distributed load q , which could be equivalent to three
917 nodal loads $F = ql/4$. The top four components and the two compressive bars are made from
918 concrete materials, while the inner two elements and the bottom three tension bars are of steel
919 materials. The displacement of point O can be analytically constructed by

$$d_o = \frac{ql^2}{2} \left(\frac{3.81}{A_c E_c} + \frac{1.13}{A_s E_s} \right) \quad (78)$$

where the model parameters in Eq. (78) are listed in Table 5.

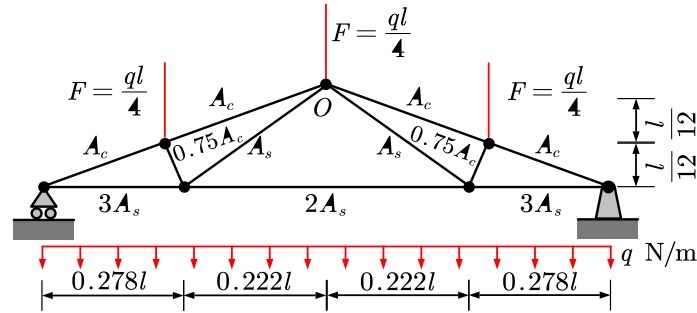


Fig. 20. A roof truss structure [6].

Table 5

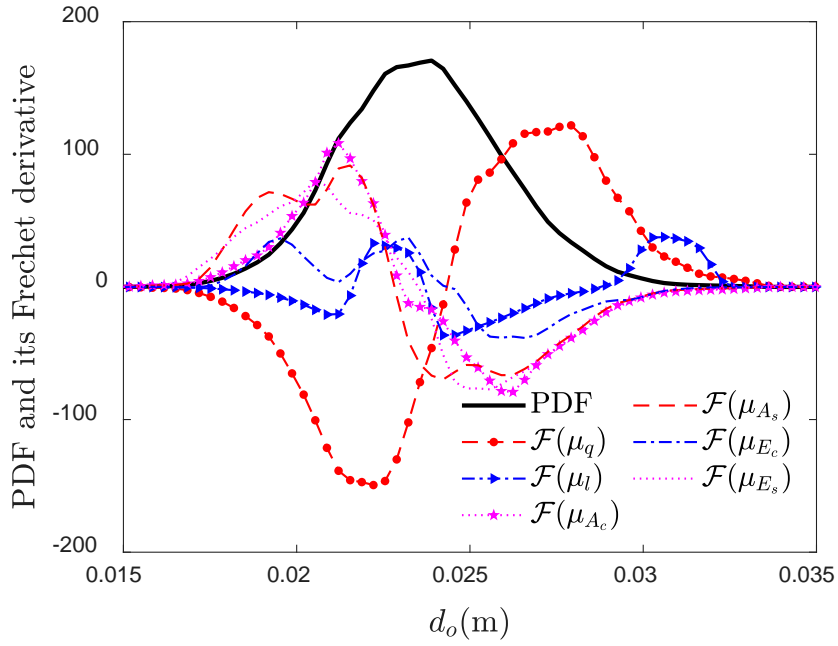
Model parameters of the roof truss structure [6].

Parameters	Distribution	Mean	C.O.V.	Physical meanings
q (N/m)	Normal	20,000	0.07	Uniform load
l (m)	Normal	12	0.01	Length of component
A_c (m ²)	Normal	0.04	0.12	Sectional area of concrete
A_s (m ²)	Normal	9.82×10^{-4}	0.06	Sectional area of steel
E_c (N/m ²)	Normal	2×10^{10}	0.06	Modulus of elasticity of concrete
E_s (N/m ²)	Normal	1×10^{11}	0.06	Modulus of elasticity of steel

Note: C.O.V. is the abbreviation of coefficient of variation.

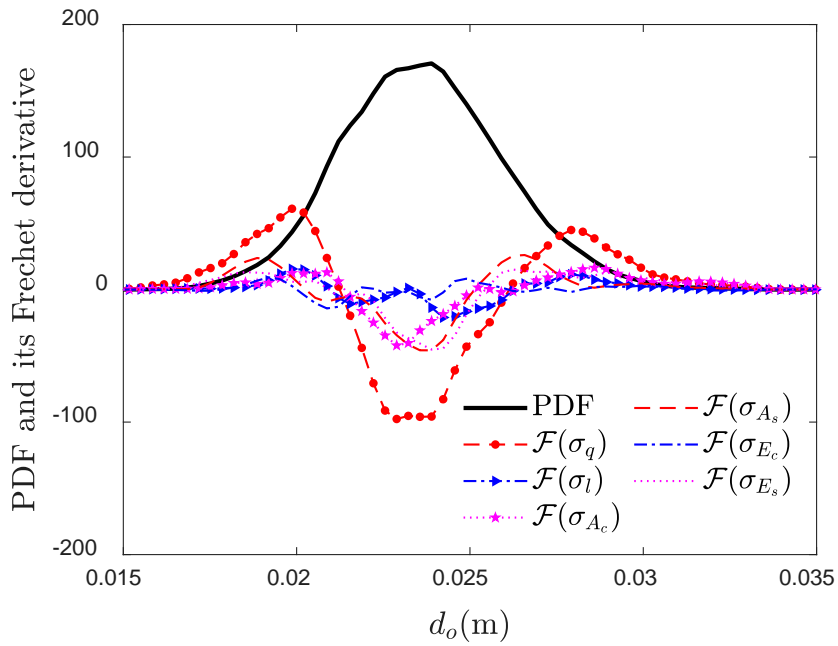
Though the normal distribution is not perfectly physically consistent with the above parameters, in the present case it is still appropriate because the standard deviation (calculated by C.O.V.) is relatively small, therefore it is almost impossible to generate negative values that have no physical sense.

934 Numerical results of the GSIs in terms of the mean values of source random variables are
935 shown in Fig. 21 while pictured in Fig. 22 are the GSIs in terms of the standard deviations of
936 source random variables. It is seen that in terms of the mean values of source random variables,
937 the order of importance is $F(\mu_q) > F(A_c) \approx F(\mu_{E_c}) \approx F(\mu_{A_s}) \approx F(\mu_{E_s}) > F(\mu_l)$, where
938 $F(\mu_q)$ is the GSI in terms of μ_q and similar symbols apply to other GSIs. In terms of the
939 standard deviations of source random variables, it is found that the rule of GSIs in terms of the
940 standard deviations of source random variables are more complex compared to those in terms
941 of the means of source random variables. This is consistent with the discussions in Example 1.
942 It should be emphasized that these orders are qualitative, while the quantitative information
943 shown in Figs. 21 and 22 can be adopted for more rational decision-making or employed in
944 reliability-based structural optimization. For instance, it is seen from Fig. 22 that the GSIs in
945 terms of σ_l and σ_{E_c} are much smaller compared to the GSIs in terms of the standard
946 deviations of the other source random variables. This means that, if a decision-making is needed
947 whether the epistemic uncertainty in the standard deviations of source random variables are
948 needed, then it can be such decided that the effects of epistemic uncertainty in the standard
949 deviations of l and E_c can be ignored, and thus the involved factors in terms of epistemic
950 uncertainty in the problem can be reduced.



951

952 **Fig. 21.** Fréchet-derivative-based GSI in terms of mean values for Example 5.



953

954 **Fig. 22.** Fréchet-derivative-based GSI with respect to standard deviations for Example 5.

955

956 **6 Concluding Remarks**

957 In the present paper, for the systems involving random parameters, starting from a

958 functional perspective, a Fréchet-derivative-based global sensitivity index is proposed. Highly

959 efficient numerical algorithms are elaborated by incorporating the probability density evolution
960 method and the change of probability measure (PDEM-COM algorithm). The main findings
961 and conclusions are:

962 (1) The proposed sensitivity defined by the Fréchet derivative, i.e., the change of the PDF
963 of the output QoI in terms of the change of the PDF of the input basic random variables is
964 essentially a global sensitivity index. Compared to the traditional sensitivity indices, e.g., the
965 Sobol' indices and the moment-independent IMs, the proposed GSI is more informative and
966 flexible by providing not only the magnitude of change at the level of the PDF, but also the
967 direction of effects being positive or adverse.

968 (2) The PDEM-COM algorithm by incorporating the probability density evolution method
969 (PDEM) and the change of probability measure (COM) provides a highly efficient and fairly
970 accurate tool for the evaluation of the proposed GSI in terms of the distribution parameters of
971 input random variables.

972 (3) Numerical examples, including two analytical and three engineering cases, are
973 extensively studied, demonstrating the accuracy and effectiveness of the proposed GSI as well
974 as the PDEM-COM algorithm.

975 Some important and interesting issues for extension shall be studied further, including,
976 e.g., how to apply the present GSI for dependent source random variables and subsets of
977 variables, etc.

978

979 **Acknowledgement**

980 Financial supports from the National Natural Science Foundation of China (NSFC Grant
981 Nos. 51725804, 51538010 and 11761131014), the DFG Grant No. 392113882, the NSFC-
982 Guangdong Province Joint Project (Grant No. U1711264) are highly appreciated. The China
983 Scholarship Council (CSC) is gratefully appreciated by the second author.

984

985 **Appendix A. A Proposition on Fréchet-Derivative-based GSI**

986 The following proposition in terms of the Fréchet-derivative-based GSI is stated and
 987 proved.

988 **Proposition.** *The definition in Eq. (31) in a parametric form allows that*

$$989 \quad \|\delta \tilde{p}_X - \delta p_X\| \leq \|\delta \tilde{p}_\Theta - \delta p_\Theta\|_V \cdot \sup_{0 \leq t \leq 1} \|\mathbf{F}_\psi(p_\Theta + t\delta \tilde{p}_\Theta + (1-t)\delta p_\Theta)\| \quad (79)$$

990 holds, where $\delta \tilde{p}_X$ is the variation of \tilde{p}_X due to an arbitrary variation of p_Θ by $\delta \tilde{p}_\Theta$,
 991 while δp_X is the variation of p_X due to a parametric variation of p_Θ by δp_Θ . It
 992 indicates that the variation of the output PDF is a.e. the same no matter the input PDF is
 993 parametric or not, as long as the variation of the input PDF is sufficiently small.

994 **Proof.** Denote

$$995 \quad \begin{cases} \delta \tilde{p}_X = \psi(p_\Theta + \delta \tilde{p}_\Theta) - \psi(p_\Theta), \\ \delta p_X = \psi(p_\Theta + \delta p_\Theta) - \psi(p_\Theta), \end{cases} \quad (80)$$

996 and

$$997 \quad \delta \tilde{p}_X - \delta p_X = \psi(p_\Theta + \delta \tilde{p}_\Theta) - \psi(p_\Theta + \delta p_\Theta). \quad (81)$$

998 According to the mean value theorem [24], we have

$$999 \quad \begin{aligned} \|\delta \tilde{p}_X - \delta p_X\| &= \|\psi(p_\Theta + \delta \tilde{p}_\Theta) - \psi(p_\Theta + \delta p_\Theta)\| \\ &\leq \|\delta \tilde{p}_\Theta - \delta p_\Theta\|_V \cdot \sup_{0 \leq t \leq 1} \|\mathbf{F}_\psi(p_\Theta + t\delta \tilde{p}_\Theta + (1-t)\delta p_\Theta)\| \end{aligned} \quad (82)$$

1000 where \mathbf{F}_ψ is the Fréchet derivative of ψ . ■

1001

1002 **Appendix B. Analytical Expressions of the Norm Term of GSI for**

1003 **Some Common Distributions**

1004 The norm term in the proposed Fréchet-derivative-based GSI in Eq. (31) is defined as

$$1005 \quad \left\| \frac{\partial p_{\Theta}(\theta; \xi)}{\partial \xi_j} \right\|_V = \frac{1}{2} \int_{\Omega_{\Theta}} \left| \frac{\partial p_{\Theta}(\theta; \xi)}{\partial \xi_j} \right| d\theta, \quad j = 1, 2, \dots, m \quad (83)$$

1006 where ξ is the distribution parameter of the input PDF $p_{\Theta}(\theta; \xi)$. This defined norm can be
 1007 exactly evaluated for some common distributions, and the results are summarized as follows.

$$1008 \quad (1) \text{ Normal distribution } p_{\Theta}(\theta; \mu, \sigma) = \frac{1}{\sqrt{2\pi}\sigma} e^{-\frac{(\theta-\mu)^2}{2\sigma^2}} \text{ for } \theta \in \mathbb{R}.$$

1009 A normal distribution with the mean value μ and the standard deviation σ has the
 1010 explicitly defined norms by

$$1011 \quad \left\{ \begin{aligned} \left\| \frac{\partial p_{\Theta}(\theta; \mu, \sigma)}{\partial \mu} \right\|_V &= \frac{1}{2} \int_{-\infty}^{+\infty} \left| \frac{\theta - \mu}{\sigma^2} \frac{1}{\sqrt{2\pi}\sigma} e^{-\frac{(\theta-\mu)^2}{2\sigma^2}} \right| d\theta = \frac{1}{\sqrt{2\pi}\sigma}, \\ \left\| \frac{\partial p_{\Theta}(\theta; \mu, \sigma)}{\partial \sigma} \right\|_V &= \frac{1}{2} \int_{-\infty}^{+\infty} \left| \frac{(\theta - \mu)^2 - \sigma^2}{\sigma^3} \frac{1}{\sqrt{2\pi}\sigma} e^{-\frac{(\theta-\mu)^2}{2\sigma^2}} \right| d\theta = \frac{2}{\sqrt{2\pi}\sigma} e^{-1/2}. \end{aligned} \right. \quad (84)$$

$$1012 \quad (2) \text{ Log-normal distribution } p_{\Theta}(\theta; \alpha, \beta) = \frac{1}{\sqrt{2\pi}\beta\theta} e^{-\frac{(\ln\theta-\alpha)^2}{2\beta^2}} \text{ for } \theta > 0.$$

1013 The derivatives of the function $p_{\Theta}(\theta; \alpha, \beta)$ in terms of the parameters α and β have
 1014 explicit forms, therefore the norms are computed by

$$1015 \quad \left\{ \begin{aligned} \left\| \frac{\partial p_{\Theta}(\theta; \alpha, \beta)}{\partial \alpha} \right\|_V &= \frac{1}{2} \int_0^{+\infty} \left| \frac{\ln\theta - \alpha}{\beta^2} \frac{1}{\sqrt{2\pi}\beta\theta} e^{-\frac{(\ln\theta-\alpha)^2}{2\beta^2}} \right| d\theta = \frac{1}{\sqrt{2\pi}\beta}, \\ \left\| \frac{\partial p_{\Theta}(\theta; \alpha, \beta)}{\partial \beta} \right\|_V &= \frac{1}{2} \int_0^{+\infty} \left| \frac{(\ln\theta - \alpha)^2 - \beta^2}{\beta^3} \frac{1}{\sqrt{2\pi}\beta\theta} e^{-\frac{(\ln\theta-\alpha)^2}{2\beta^2}} \right| d\theta = \frac{2}{\sqrt{2\pi}\beta} e^{-1/2}. \end{aligned} \right. \quad (85)$$

1016 For the norm of some other distributions, the numerical computation on the derivative as
 1017 well as the integral is recommended.

1018

1019 **Appendix C. Analytical Expressions of GSI in Example 2**

1020 (1) Subcase 1

1021 Theoretically, X is also normally distributed with the mean value $\mu = \mu_1 + 2\mu_2$ and the

1022 standard deviation $\sigma = \sqrt{\sigma_1^2 + 4\sigma_2^2}$, therefore the PDF of X is

$$1023 \quad p_X(x) = \frac{1}{\sqrt{2\pi(\sigma_1^2 + 4\sigma_2^2)}} \exp\left\{-\frac{(x - \mu_1 - 2\mu_2)^2}{2(\sigma_1^2 + 4\sigma_2^2)}\right\}. \quad (86)$$

1024 Then, taking derivatives of Eq. (86) with respect to μ_1 , μ_2 , σ_1 and σ_2 , we have

$$1025 \quad \frac{\partial p_X}{\partial \mu_1} = \frac{(x - \mu_1 - 2\mu_2)}{\sqrt{2\pi(\sigma_1^2 + 4\sigma_2^2)^{3/2}}} \exp\left\{-\frac{(x - \mu_1 - 2\mu_2)^2}{2(\sigma_1^2 + 4\sigma_2^2)}\right\}, \quad (87)$$

$$1026 \quad \frac{\partial p_X}{\partial \mu_2} = \frac{2(x - \mu_1 - 2\mu_2)}{\sqrt{2\pi(\sigma_1^2 + 4\sigma_2^2)^{3/2}}} \exp\left\{-\frac{(x - \mu_1 - 2\mu_2)^2}{2(\sigma_1^2 + 4\sigma_2^2)}\right\}, \quad (88)$$

$$1027 \quad \frac{\partial p_X}{\partial \sigma_1} = \frac{\sigma_1}{\sqrt{2\pi}} \exp\left\{-\frac{(x - \mu_1 - 2\mu_2)^2}{2(\sigma_1^2 + 4\sigma_2^2)}\right\} \cdot \frac{(x - \mu_1 - 2\mu_2)^2 - (\sigma_1^2 + 4\sigma_2^2)}{(\sigma_1^2 + 4\sigma_2^2)^{5/2}}, \quad (89)$$

1028 and

$$1029 \quad \frac{\partial p_X}{\partial \sigma_2} = \frac{4\sigma_2}{\sqrt{2\pi}} \exp\left\{-\frac{(x - \mu_1 - 2\mu_2)^2}{2(\sigma_1^2 + 4\sigma_2^2)}\right\} \cdot \frac{(x - \mu_1 - 2\mu_2)^2 - (\sigma_1^2 + 4\sigma_2^2)}{(\sigma_1^2 + 4\sigma_2^2)^{5/2}}. \quad (90)$$

1030 Integrating Eqs. (87) to (90) in the failure domain $\Omega_f : X < x_{\text{lim}}$ leads to

$$1031 \quad \frac{\partial P_X}{\partial \mu_1} = \frac{1}{\sqrt{2\pi(\sigma_1^2 + 4\sigma_2^2)}} \exp\left\{-\frac{(x_{\text{lim}} - \mu_1 - 2\mu_2)^2}{2(\sigma_1^2 + 4\sigma_2^2)}\right\}, \quad (91)$$

$$1032 \quad \frac{\partial P_X}{\partial \mu_2} = \frac{2}{\sqrt{2\pi(\sigma_1^2 + 4\sigma_2^2)}} \exp\left\{-\frac{(x_{\text{lim}} - \mu_1 - 2\mu_2)^2}{2(\sigma_1^2 + 4\sigma_2^2)}\right\}, \quad (92)$$

$$1033 \quad \frac{\partial P_X}{\partial \sigma_1} = \frac{\sigma_1(x_{\text{lim}} - \mu_1 - 2\mu_2)}{\sqrt{2\pi(\sigma_1^2 + 4\sigma_2^2)^{3/2}}} \exp\left\{-\frac{(x_{\text{lim}} - \mu_1 - 2\mu_2)^2}{2(\sigma_1^2 + 4\sigma_2^2)}\right\}, \quad (93)$$

1034 and

$$1035 \quad \frac{\partial P_x}{\partial \sigma_2} = \frac{4\sigma_2(x_{\text{lim}} - \mu_1 - 2\mu_2)}{\sqrt{2\pi}(\sigma_1^2 + 4\sigma_2^2)^{3/2}} \exp\left\{-\frac{(x_{\text{lim}} - \mu_1 - 2\mu_2)^2}{2(\sigma_1^2 + 4\sigma_2^2)}\right\}. \quad (94)$$

1036 Eqs. (91) to (94) are exactly the Fréchet derivatives of failure probability in terms of the
1037 distribution parameters of input basic random variables, where the norm terms are omitted for
1038 simplicity but all are available in [Appendix B](#).

1039 (2) Subcase 2

1040 For μ_1 and μ_2 , there is:

$$1041 \quad \text{(a)} \quad \frac{\partial p_{x_a}}{\partial \mu_1} = \frac{\partial p_{x_a}}{\partial \mu_2} = \frac{(x - \mu_1 - \mu_2)}{\sqrt{2\pi}(\sigma_1^2 + \sigma_2^2)^{3/2}} \exp\left\{-\frac{(x - \mu_1 - \mu_2)^2}{2(\sigma_1^2 + \sigma_2^2)}\right\},$$
$$1042 \quad \text{(b)} \quad \frac{\partial p_{x_b}}{\partial \mu_1} = -\frac{\partial p_{x_b}}{\partial \mu_2} = \frac{(x - \mu_1 + \mu_2)}{\sqrt{2\pi}(\sigma_1^2 + \sigma_2^2)^{3/2}} \exp\left\{-\frac{(x - \mu_1 + \mu_2)^2}{2(\sigma_1^2 + \sigma_2^2)}\right\}. \quad (95)$$

1043 For σ_1 and σ_2 , there is:

$$1044 \quad \text{(a)} \quad \frac{\partial p_{x_a}}{\partial \sigma_{1,2}} = \frac{\sigma_{1,2}}{\sqrt{2\pi}} \exp\left\{-\frac{(x - \mu_1 - \mu_2)^2}{2(\sigma_1^2 + \sigma_2^2)}\right\} \cdot \frac{(x - \mu_1 - \mu_2)^2 - (\sigma_1^2 + \sigma_2^2)}{(\sigma_1^2 + \sigma_2^2)^{5/2}},$$
$$1045 \quad \text{(b)} \quad \frac{\partial p_{x_b}}{\partial \sigma_{1,2}} = \frac{\sigma_{1,2}}{\sqrt{2\pi}} \exp\left\{-\frac{(x - \mu_1 + \mu_2)^2}{2(\sigma_1^2 + \sigma_2^2)}\right\} \cdot \frac{(x - \mu_1 + \mu_2)^2 - (\sigma_1^2 + \sigma_2^2)}{(\sigma_1^2 + \sigma_2^2)^{5/2}}. \quad (96)$$

1046

1047 **References**

- 1048 [1] Saltelli A. 2002. Sensitivity analysis for importance assessment. *Risk Analysis*, 22(3): 579-590.
- 1049 [2] Sobol' I M, Kucherenko S. 2010. A new derivative based importance criterion for groups of variables
1050 and its link with the global sensitivity indices. *Computer Physics Communications*, 181: 1212-1217.
- 1051 [3] Au S K. 2005. Reliability-based design sensitivity by efficient simulation. *Computers and Structures*,
1052 83: 1048-1061.
- 1053 [4] Lu Z Z, Song S F, Yue Z F, et al. 2008. Reliability sensitivity method by line sampling. *Structural*
1054 *Safety*, 30: 517-532.
- 1055 [5] Guo J, Du X P. 2009. Reliability sensitivity analysis with random and interval variables. *International*
1056 *Journal for Numerical Methods in Engineering*, 78: 1585-1617.

- 1057 [6] Song S F, Lu Z Z, Qiao H W. 2009. Subset simulation for structural reliability sensitivity analysis.
1058 Reliability Engineering and System Safety, 94: 658-665.
- 1059 [7] Wei P F, Lu Z Z, Hao W R, et al. 2012. Efficient sampling methods for global reliability sensitivity
1060 analysis. Computer Physics Communications, 183: 1728-1743.
- 1061 [8] Wei P F, Song J W, Bi S F, et al. 2019. Non-intrusive stochastic analysis with parameterized imprecise
1062 probability models: II. Reliability and rare events analysis. Mechanical Systems and Signal
1063 Processing, 126: 227-247.
- 1064 [9] Lin J H. 1985. Sensitivity analysis in structural dynamic optimization. Vibration and Shock, 4(1): 1-
1065 6. (in Chinese)
- 1066 [10] Ryu Y S, Haririan M, Wu C C, et al. 1985. Structural design sensitivity analysis of nonlinear response.
1067 Computers and Structures, 21(1/2): 245-255.
- 1068 [11] Allaire G, Jouve F, Toader A.-M. 2004. Structural optimization using sensitivity analysis and a level-
1069 set method. Journal of Computational Physics, 194: 363-393.
- 1070 [12] Choi K K, Kim N H. 2005. Structural Sensitivity Analysis and Optimization 2: Nonlinear Systems
1071 and Applications. New York: Springer Science + Business Media.
- 1072 [13] Sobol' I M. 1993. Sensitivity estimates for nonlinear mathematical models. Mathematical Modeling
1073 and Computational Experiment, 1(4): 407-414.
- 1074 [14] Homma T, Saltelli A. 1996. Importance measures in global sensitivity analysis of nonlinear models.
1075 Reliability Engineering and System Safety, 52: 1-17.
- 1076 [15] Chun M-H, Han S-J, Tak N-IL. 2000. An uncertainty importance measure using a distance metric for
1077 the change in a cumulative distribution function. Reliability Engineering and System Safety, 70: 313-
1078 321.
- 1079 [16] Borgonovo E. 2007. A new uncertainty importance measure. Reliability Engineering and System
1080 Safety, 92: 771-784.
- 1081 [17] Borgonovo E, Castaings W, Tarantola S. 2011. Moment independent importance measures: New
1082 results and analytical test cases. Risk Analysis, 31(3): 404-428.
- 1083 [18] Chen J B, Li J. 2008. Global sensitivity in nonlinear stochastic dynamic response analysis of structures.
1084 Chinese Journal of Computational Mechanics, 25(2): 169-176. (in Chinese)
- 1085 [19] Sudret B. 2008. Global sensitivity analysis using polynomial chaos expansions. Reliability
1086 Engineering and System Safety, 93(7): 964-979.
- 1087 [20] Blatman G, Sudret B. 2010. Efficient computation of global sensitivity indices using sparse
1088 polynomial chaos expansions. Reliability Engineering and System Safety, 95: 1216-1229.
- 1089 [21] Grigoriu M. 2002. Stochastic Calculus: Application in Science and Engineering. New York: Springer
1090 Science + Business Media.
- 1091 [22] Bobrowski A. 2005. Functional Analysis for Probability and Stochastic Processes: An Introduction.
1092 London: Cambridge University Press.

- 1093 [23] Curtain R. F., Zwart H. 1995. An Introduction to Infinite-Dimensional Linear Systems Theory. New
1094 York: Springer-Verlag.
- 1095 [24] Atkinson K, Han W M. 2009. Theoretical Numerical Analysis: A Functional Analysis Framework.
1096 New York: Springer Science+Business Media.
- 1097 [25] Andrews B, Hopper C. 2011. The Ricci Flow in Riemannian Geometry: A Complete Proof of the
1098 Differentiable $1/4$ -Pinching Sphere Theorem. Berlin: Springer-Verlag.
- 1099 [26] Chen J B, Wan Z Q. 2019. A compatible probabilistic framework for simultaneous aleatory and
1100 epistemic uncertainty of basic parameters of structures by synthesizing the change of measure and
1101 change of random variables. *Structural Safety*, 78: 76-87.
- 1102 [27] Li J, Chen J B. 2008. The principle of preservation of probability and the generalized density evolution
1103 equation. *Structural Safety*, 30: 65-77.
- 1104 [28] Li J, Chen J B. 2009. Stochastic Dynamics of Structures. Hoboken: John Wiley & Sons.
- 1105 [29] Feng D C, Xie S C, Deng W N, et al. 2019. Probabilistic failure analysis of reinforced concrete beam-
1106 column sub-assembly under column removal scenario. *Engineering Failure Analysis*, 100: 381-392.
- 1107 [30] Chen J B, Zhang S H. 2013. Improving point selection in cubature by a new discrepancy. *SIAM
1108 Journal on Scientific Computing*, 35(5): A2121-A2149.
- 1109 [31] Chen J B, Yang J Y, Li J. 2016. A GF-discrepancy for point selection in stochastic seismic response
1110 analysis of structures with uncertain parameters. *Structural Safety*, 59: 20-31.
- 1111 [32] Chen J B, Chan J P. 2019. Error estimate of point selection in uncertainty quantification of nonlinear
1112 structures involving multiple nonuniformly distributed parameters. *International Journal for
1113 Numerical Methods in Engineering*, 118: 536–560.
- 1114 [33] Li J, Chen J B. 2006. Dimension-reduction strategy via mapping for probability density evolution
1115 analysis of nonlinear stochastic systems. *Probabilistic Engineering Mechanics*, 21: 442-453.
- 1116 [34] Jiang Z M, Li J. 2017. High dimensional structural reliability with dimension reduction. *Structural
1117 Safety*, 69: 35-46.
- 1118 [35] Li J, Chen J B. 2004. Probability density evolution method for dynamic response analysis of structures
1119 with uncertain parameters. *Computational Mechanics*, 34: 400-409.
- 1120 [36] Fan W L, Ang A H-S. 2017. Reliability assessment of deteriorating structures using Bayesian updated
1121 probability density evolution method (PDEM). *Structural Safety*, 65: 60-73.
- 1122 [37] Wang Y. 2012. Uncertain parameters sensitivity in Monte Carlo Simulation by Sample reassembling.
1123 *Computers and Geotechnics*, 46: 39-47.
- 1124 [38] Wei P F, Lu Z Z, Song J W. 2014. Extended Monte Carlo Simulation for parametric global sensitivity
1125 analysis and optimization. *AIAA Journal*, 52(4): 867-878.
- 1126 [39] Jiang Z M, Li J. 2016. Analytical solutions of the generalized probability density evolution equation
1127 of three classes stochastic systems. *Chinese Journal of Theoretical and Applied Mechanics*, 48(2):
1128 413-421. (In Chinese).

- 1129 [40] Izenman A J. 2008. Modern Multivariate Statistical Techniques: Regression, Classification and
1130 Manifold Learning. New York: Springer-Verlag.
- 1131 [41] Zhao Y G, Zhang X Y, Lu Z H. 2018. Complete monotonic expression of the fourth-moment normal
1132 transformation for structural reliability. Computers and Structures, 196: 186-199.
- 1133 [42] Valdebenito M A, Jensen H A, Hernández H B, et al. 2018. Sensitivity estimation of failure probability
1134 applying line sampling. Reliability Engineering and System Safety, 171: 99-111.
- 1135 [43] Breitung K W. 1994. Asymptotic Approximations for Probability Integrals. Berlin: Springer-Verlag.
- 1136 [44] Tao W F, Li J. 2017. An ensemble evolution numerical method for solving generalized density
1137 evolution equation. Probabilistic Engineering Mechanics, 48: 1-11.
- 1138 [45] Eldred M S, Agarwal H, Perez V M, et al. 2007. Investigation of reliability method formulations in
1139 DAKOTA/UQ. Structure and Infrastructure Engineering, 3(3): 199-213.
- 1140 [46] Royset J O, Der Kiureghian A, Polak E. 2001. Reliability-based optimal structural design by the
1141 decoupling approach. Reliability Engineering and System Safety, 73: 213-221.
- 1142 [47] Dubourg V, Sudret B, Bourinet J.-M. 2011. Reliability-based design optimization using kriging
1143 surrogates and subset simulation. Structural and Multidisciplinary Optimization, 44(5): 673-690.
- 1144 [48] Moustapha M, Sudret B. 2019. Surrogate-assisted reliability-based design optimization: a survey and
1145 a unified modular framework. Structural and Multidisciplinary Optimization, 60:2157-2176.